Copyright Warning & Restrictions

The copyright law of the United States (Title 17, United States Code) governs the making of photocopies or other reproductions of copyrighted material.

Under certain conditions specified in the law, libraries and archives are authorized to furnish a photocopy or other reproduction. One of these specified conditions is that the photocopy or reproduction is not to be "used for any purpose other than private study, scholarship, or research." If a, user makes a request for, or later uses, a photocopy or reproduction for purposes in excess of "fair use" that user may be liable for copyright infringement,

This institution reserves the right to refuse to accept a copying order if, in its judgment, fulfillment of the order would involve violation of copyright law.

Please Note: The author retains the copyright while the New Jersey Institute of Technology reserves the right to distribute this thesis or dissertation

Printing note: If you do not wish to print this page, then select "Pages from: first page # to: last page #" on the print dialog screen

ABSTRACT

NOVEL EXPERIMENTAL METHOD FOR THE DETERMINATION OF THE MINIMUM AGITATION SPEED FOR SOLIDS SUSPENSION IN FLAT-BOTTOMED STIRRED TANK REACTORS

By

Shriarjun Shastry

Knowledge of the minimum agitation speed, N_{js}, required to suspend finely divided solids in vessels stirred by an impeller is a critical parameter to properly operate industrial tanks in a large number of industrial operations. The most common experimental approach to measure N_{js} is that of Zwietering's (*Chem. Eng. Sci.*, 1958, **8,** 244-253), consisting of visually inspecting the tank bottom and visually determining the impeller agitation speed at which the solids are observed to rest on the tank bottom for no more than 1-2 seconds before being swept away. This method is quite reliable, but a method not relying on the operator would clearly be preferred. Therefore, the main objective of this work was to develop a simple, repeatable, and observer-independent method to determine N_{js} for a variety of agitation systems and agitation conditions in tanks with a flat-bottom, the most common tank shape for which N_{js} has been obtained in previous studies. Flat bottom reactors are also among the most widely used reactors for research and development studies in the pharmaceutical and biopharmaceutical industry.

In this study, N_{js} was experimentally determined by using a newly developed method in which the area covered by the unsuspended solids still at the bottom of the tank was measured at increasing agitation speeds, starting at low speeds (below N_{js}). To do so, images of the tank bottom were captured in .jpg format by a digital camera. Each image was processed with the appropriate software (Image J) to quantitatively determine

the area still covered by solids at that speed. Increasing the agitation speed increased the amount of solids being suspended, resulting in a decrease in the area covered by solids at the bottom of the tank. Plots of the area covered by the solids vs. the corresponding agitation speed resulted in a linear function, which when extrapolated to $A \rightarrow 0$ yielded the expected value of N_{js} (named $N_{js\text{-}A}$). The values so obtained for $N_{js\text{-}A}$ were then compared to the N_{js} value determined visually ($N_{js\text{-}vis}$).

This approach was tested for a number of mixing systems with different impeller types (disk turbines, flat-blade turbine, pitched-baled turbines, hydrofoil impeller), impeller off-bottom clearances, impeller sizes, and tanks sizes. Preliminary tests were conducted using the same method but in hemispherical tanks, where the solids at the bottom of the tank a formed an approximate circular pattern. As compared to hemispherical bottomed tank, the solid particles in flat-bottomed tanks were dispersed all over the bottom of the tank. Therefore, the sum of all the individual areas covered by the solid particles deposited at the bottom was quantitatively determined. The results for $N_{js\text{-}A}$ obtained with the new method were compared with those obtained using the traditional Zwietering's approach. In general, excellent agreement was found between $N_{js\text{-}A}$ and $N_{js\text{-}vis}$. It can be concluded that this newly developed method constitutes a novel, reliable, and, especially, *observer-independent* method to experimentally determine N_{js}.

It is expected that this approach could be of particular relevance in a variety of mixing applications, including the suspension of micro-carrier particles, such as glass beads, on to which animal cells can become attached and used to produce various bio-products, and in the suspension of beads for production of proteins.

NOVEL EXPERIMENTAL METHOD FOR THE DETERMINATION OF THE MINIMUM AGITATION SPEED FOR SOLIDS SUSPENSION IN FLAT-BOTTOMED STIRRED TANK REACTORS

by
Shriarjun Shastry

A Thesis
Submitted to the Faculty of
New Jersey Institute of Technology
in Partial Fulfillment of the Requirements for the Degree of
Master of Science in Biopharmaceutical Engineering

Otto H. York Department of Chemical, Biological and Pharmaceutical Engineering

January 2017

APPROVAL PAGE

NOVEL EXPERIMENTAL METHOD FOR THE DETERMINATION OF THE MINIMUM AGITATION SPEED FOR SOLIDS SUSPENSION IN FLAT-BOTTOMED STIRRED TANK REACTORS

Shriarjun Shastry

Dr. Piero M. Armenante, Thesis Advisor Date
Distinguished Professor of Chemical, Biological and Pharmaceutical Engineering, NJIT

Dr. Laurent Simon, Committee Member Date
Associate Professor of Chemical, Biological and Pharmaceutical Engineering, NJIT

Dr. Michael A. Hanson, Committee Member Date
Adjunct Professor of Chemical, Biological and Pharmaceutical Engineering, NJIT

BIOGRAPHICAL SKETCH

Author: Shriarjun Shastry

Degree: Master of Science

Date: January 2017

Undergraduate and Graduate Education:

- Master of Science in Biopharmaceutical Engineering,
- New Jersey Institute of Technology, Newark, NJ

- Bachelor of Engineering in Biotechnology,
- B. V. Bhoomaraddi College of Engineering and Technology, Hubli, India

Major: Biopharmaceutical Engineering

To My Family and Friends

ACKNOWLEDGMENT

I have taken efforts to complete this study. However, it would not have been possible without the kind support and help of many individuals and organizations. I would like to extend my sincere thanks to all of them.

I am highly indebted to Dr. Piero M. Armenante for his guidance and constant supervision, as well as for providing necessary information & support in completing the project. Also, I like to thank Dr. Laurent Simon and Dr. Michael A. Hanson for their continuous support and guidance throughout the course of this project work**.**

My deepest gratitude to my parents & members of my family for their kind co-operation and encouragement, which helped me in completion of this study.

TABLE OF CONTENTS

TABLE OF CONTENTS

LIST OF TABLES

Table **Page**

.

LIST OF FIGURES

LIST OF FIGURES
(Continued)

Figure **Page**

NOMENCLATURE

D	Impeller diameter (mm)
T	Tank diameter (mm)
H	Liquid height (mm)
C_b	Bottom clearance (mm)
N	Rotational speed (rpm)
N_{js}	Minimum agitation speed for solid suspension
P	Dissipation power (watt)
τ	Torque (Nm)

CHAPTER 1

INTRODUCTION

1.1 Background Introduction

The suspension of solid particles in liquid in a stirred tank occurs in a wide variety of processes from crystallization to ore processing. Down-pumping, mixed or axial impellers have been reported to be the most efficient geometries for suspending solids, while radial impellers require substantially higher power to achieve suspension. Radial impellers are, however, still relevant in solid-liquid mixing since this impeller geometry is efficient for gas-liquid dispersion, and many such systems also contain solids such as in aerobic fermentation and activated sludge treatment. The curved blade impeller has gained popularity as an alternative to the Rushton due to its efficiency in gas-liquid dispersion as the shape of the curve eliminates or minimizes the formation of cavities that lead to substantial drop in power.

In agitated vessels, the degree of solid suspension is generally classified into three levels: on-bottom motion, complete off-bottom suspension, and uniform suspension (Paul et al., 2004). For many applications, it is often important just to provide enough agitation to completely suspend the solids off the tank bottom. Below this off-bottom particle suspension state, the total solid-liquid interfacial surface area is not completely or efficiently utilized. Therefore, it is important to be able to determine the impeller agitation speed N_{js}, at which the just suspended state is achieved by the particles (Armenante and Uehara-Nagamine 1998). Although N_{js} has been obtained for a number of mixing systems, very little information is available in the literature for the solid

suspension in the system most commonly used in pharmaceutical industry, as well as bio-pharmaceutical industries.

Homogeneous large-scale cultivation of anchorage dependent animal cells for the production of therapeutic protein is made possible by cultivating the cells on small solid spherical particles called micro-carriers, which are suspended in growth medium. This system also requires suspension of beads as a whole. And determination of N_{js} is very important.

1.2 Objectives of This Work

The typical method to measure experimentally N_{js} is that of Zwietering's (1958). Accordingly, N_{js} is obtained by visually inspecting the tank bottom and visually determining the impeller agitation speed at which the solids are observed to rest on the tank bottom for no more than 1-2 seconds before being swept away. Although this method is quite reliable, there is clearly the need to develop a method that is not observer-based. In the previous study performed in this laboratory, Anqi Zhou and Yingxi Tang experimentally developed a new method to determine the minimum agitation speed, N_{js}, for just solid suspension in a hemispherical bottomed tank and torispherical bottomed tank. The approached used Anqi Zhou was based on the determination of the area still covered by solids at progressively higher agitation speeds from which N_{js} could be obtained. However, this method relied on the determination of the solids area using a grid marking at the bottom of the vessel from which the solids area could be measured. This method was conceptually valid but somewhat impractical. In addition, it was applicable only to hemispherical- and torispherical-bottomed tanks where the solids formed a round or elliptical shape contour. This approach failed when flat-

bottom tanks were used since the solids were scattered along the tank bottom forming pockets. Yingxi Tang used a similar conceptual approach but used instead computerized images of the tank bottom for her analysis, which was also limited to hemispherical bottom tanks. There is clearly a need to generate an observer-independent method that applies to flat-bottom tanks where there is no circular deposition of solid.

Therefore, the objective of this work is to develop a novel observer-independent method for the experimental determination of N_{js} in flat-bottomed tanks. This was achieved here by using a method similar to that used by Yingxi Tang who completed thesis in this lab, i.e., based on the analysis of computerized images of the tank bottom to measure the area of the solids deposited at the bottom of the tank at increasing values of the agitation speed, N, plotting N vs. the area of this region, and then linearly regressing the data to obtain N_{js} as the limit of the N value for A_S going to zero.

Once this approach was validated, it was extended to determine N_{js} for flat bottomed tank using different types of impellers to determine whether the method was still valid for different impellers generating different mixing patterns and thus solids patterns at the bottom of the tank. The novel method proposed here generated $N_{js\text{-}As}$ values that compared very favorably with the N_{js} method obtained with Zwietering method.

CHAPTER 2

EXPERIMENTAL APPARATUS, MATERIALS, AND METHODS

2.1 Apparatus

2.1.1 Flat-Bottom Mixing Vessel and Impellers

A flat-bottomed tank, frequently utilized in the pharmaceutical industry was used. The basic dimensions of this tank, shown in Figure 2.1 (a), were as follows:

Tank 1:

- Internal diameter (T): 270 mm
- Overall height: 540 mm

The tank was placed on a plastic board and raised to the required height using 2 laboratory jacks. This set up can be seen in the Figure 2.1(a). The plastic glass was transparent so that the tank bottom could be seen clearly in order to image of the same. The tank was provided with 4 baffles 20mm in width and was considered a fully baffled system. The mixing tank was filled with water so that the liquid level, H, was equal to the tank diameter (H/T = 1), corresponding to a liquid volume, V, of 15.458 liters.

The distance between the two opposite baffles was measured at the bottom of the tank, for analysis of particles of solid present at the bottom; this was a requirement so as to set up the software for determining area of solids. This is clearly shown in Figure 2.1(b).

Experiments in this system were conducted under variety of configurations, including different impellers, C/T, D/T, tank size, baffling system, and solid particle size.

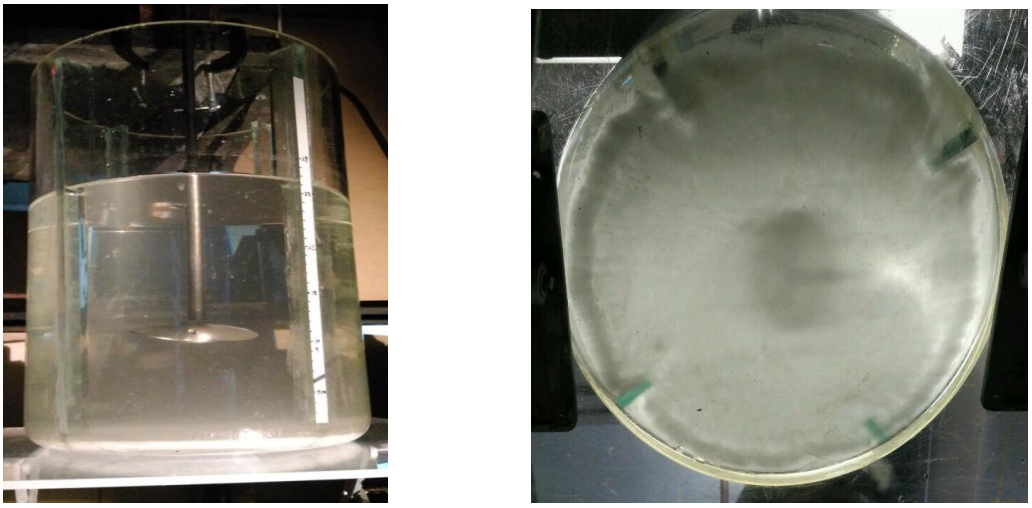

(a) (b)

Figure 2.1 (a) Flat-bottom glass-lined tank system; (b) Bottom view of the tank bottom.

Tanks for scale up studies:

Two other tanks of different sizes were also used to perform the scale up studies.

The basic dimensions of these tanks were as follows:

Tank 2:

- Internal Diameter (T): 305 mm
- Overall height: 730 mm

Tank 3:

- Internal Diameter (T): 585mm
- Overall height: 620 mm

Five types of impellers were used in these systems, as shown in Figures 2.2(a) to (e). Most experiments were conducted with a scaled-down version, used in the pharmaceutical industry and biopharmaceutical industry (Figure 2.2). The following are the impeller dimensions measured with a caliper:

First impeller: Disk Turbine

impeller diameter (D) = 100 mm, 135mm, 150mm;

height of the blade = 25.4 mm;

thickness of the blade = 12.7 mm; and

an impeller diameter-to-tank diameter ratio, D/T, of 0.22, 0.33 & 0.59.

Second impeller: Pitch Blade Turbine

impeller diameter (D) = 100 mm, 60mm;

height of the blade = 25.4 mm;

thickness of the blade = 12.7 mm; and

an impeller diameter-to-tank diameter ratio, D/T, of 0.22 & 0.33.

Third impeller: Flat blade turbine

impeller diameter (D) = 100 mm;

height of the blade = 25.4 mm;

thickness of the blade = 12.7 mm; and

an impeller diameter-to-tank diameter ratio, D/T, of 0.33.

Forth impeller: A310

impeller diameter (D) = 100mm, 150mm & 135mm;

height of the blade = 25.4 mm;

thickness of the blade = 12.7 mm; and

an impeller diameter-to-tank diameter ratio, D/T, of 0.45, 0.5 & 0.33.

Fifth impeller: Propeller

impeller diameter (D) = 100 mm;

height of the blade = 25.4 mm;

thickness of the blade = 12.7 mm; and

an impeller diameter-to-tank diameter ratio, D/T, of 0.33.

(a)

(b)

c)

(d)

Figure 2.2 Impellers used in this work: (a) A310; (b) FBT impeller; (c) 6-PBT; (d) Propeller

(e)

Figure 2.2 Impellers used in this work: (e) DT. Impellers (c) and (e) were used in the hemispherical bottom mixing system and all impellers were used in the flat-bottom mixing system.

2.1.2 Hemispherical-Bottom Mixing Vessel and Impellers

An open glass cylindrical tank with a hemispherical bottom was also used. The total tank height for this tank was 530 mm and its internal diameter was 300 mm. The bottom section of the glass tank was 100 mm and the cylindrical section was and 430 mm, although the tank was filled with water so that the liquid level, H, was equal to the tank diameter (H/T = 1), corresponding to a liquid volume, V, of 17.1 liters. The glass tank was supported by another square glass tank which was again filled with water. This tank was operated under fully baffled condition. For the fully baffled tank, the baffles were set up using clamps and tightly attached. Two types of impellers were used in this system, i.e., a six-blade, 45º degree pitched-blade turbine (6-PBT) and a 6-blade disk turbine (DT), as shown in Figures 2.3(c) and (d).

The dimensions of the impellers are as follows: for the DT, impeller diameter D = 102.5 mm, blade height: 20.3 mm, blade length= 20.4 mm, blade thickness = 1.7 mm; for

the 6-PBT: D = 102.5 mm, blade width: 17.5 mm, blade length= 20.4 mm, blade thickness = 1.7 mm.

2.1.3 Agitation System

The selected impeller was attached to a central located shaft (diameter 12.52 mm) inside the tank, rotated by a 0.25 HP motor (Chemglass, Model CG-2033-11) controlled by an external controller (Chemglass, Model CG-2033-31), as shown in Figure 2.3.

A manual tachometer was used to measure the agitation speed. A reflective strip was attached to the impeller shaft. The tachometer was pointed to this strip and it displayed the agitation speed in rpm.

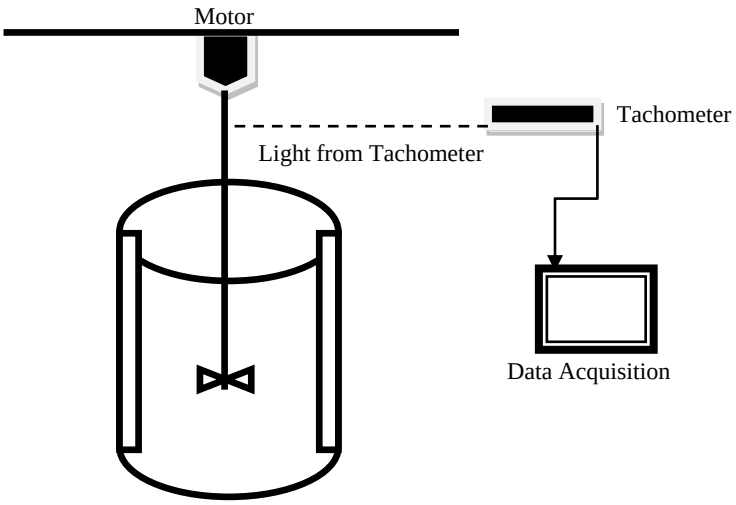

Figure 2.3 Schematic of experimental set-up of agitation system.

2.2 Materials

Tap water at room temperature was used as the liquid in all experiments. The liquid height was equal to the tank diameter in all cases.

Glass beads having average of diameters of 200 µm and 150 µm was used as the disperse phase. Prior to their use, prescreened glass beads were sieved. Four US standard screens of mesh size 40, 60, 80 and 100 were selected. 30 g of glass beads were processed at a time, by placing them in the top screen with the smallest mesh size, and shaking them for five minutes. The particles retained on the size 80 mesh screen (with an average diameter size of 200 µm) were collected separately and used in the experiments. It was noticed that the particles contained some fines, which made the suspension cloudy and required almost 15 minutes to settle down. Therefore, the fines were removed as follows. Stokes' law was used to calculate the setting time for particle size of interest.

$$V_{pt} = g\frac{(\rho_p - \rho)}{18\mu}D_p^2 \qquad \text{.....(Eqn. 1)}$$

$$t = \frac{H}{V_{pt}}$$

The setting time was calculated to be about 5 s for 200µm particles settling in a 430 mm-tall cylinder, assuming that the particle Reynolds number (Re) was less than one and drag coefficient was 24/Re. The particles were place in the cylinder with water, the system was shaken, and after 5s, the supernatant (containing the fines) was discarded. Fresh water was added and the process was repeated two more times. No fines could be observed at this point.

In most experiments, the fraction of solids was equal to 0.5% of the liquid weight (g/g), 85.5 g in hemispherical tank and 72 g in a flat bottomed tank (Tank1), respectively, as measured by an electronic scale. Also in few experiments fraction of solid used was equal to 0.75%, which is 110 g of solid. Two flat bottom tanks used for scale up studies had 110 g (Tank 2) and 660 g (Tank 3) of solids respectively.

2.3 Experimental Method to Determine Solid Suspension

In a solid suspension experiment, the tank was placed on a flat transparent plate, which rested on two lab jacks. The tank position relative to the impeller was adjusted based on the required C/T, which was varied for different set of experiments. The vessel was filled with water at the desired level was always equal to the tank diameter (H/T=1), corresponding to a liquid volume V of 17.1 liters in flat bottom tank 1, 22.2 liters in tank 2 and 107 liters in tank 3. This assembly was positioned under the impeller so that the impeller was in the vessel. The solid particles were added to the vessel where they settled. In most experiments, fully baffled (FB) systems were used, although two experiments were performed with un-baffled (UB) and two on half baffled (HB) systems (i.e., only with two baffles).

A mirror was placed below the tank at a 45-degree angle, so as to view the tank bottom. The tank bottom was illuminated using a table lamp which helped in viewing the solids at the bottom of the tank more clearly. A high quality mobile camera was placed in front of the mirror in order to take images of the tank bottom.

Agitation was started, and then progressively increased at discrete time intervals. Initially, i.e., for N=0 rpm, the particles were all resting at the bank bottom. However, as the agitation speed increased, larger fractions of the solid particles became suspended and

the area covered by the solids at the tank bottom decreased. At every new agitation speed, *N*, an image of the tank bottom was captured after the system had reached a dynamic steady state, typically after 10 seconds. Therefore, each image contained information about the fraction of solids still remaining at the tank bottom. The images were further processed to extract an observer-independent value of $N_{js\text{-}As}$ as explained below.

In addition, the visual value of N_{js} ($N_{js\text{-}visual}$) was also using Zwietering's criterion, i.e., by visually inspecting the tank bottom and visually determining the impeller agitation speed at which the solids were observed to rest on the tank bottom for no more than 1-2 seconds before being swept away.

Table 2.1 Summary of Experimental Conditions and Variable Ranges Tested in This Work.

System Variable	Flat-Bottomed Tank	Hemispherical-Bottomed Tank
Impeller Type	DT, 6-PBT, 6-FBT, Propeller, A310	DT, 6-PBT
Baffling Conditions	FB, UB, HB	FB
C_b/T	0.2, 0.25, 0.3, 0.4, 0.5	0.2, 0.3, 0.4, 0.5
Particle Size	200 μm, 150 μm	200 μm

2.4 Data Processing and Analysis for the Novel Determination of N_{js} ($N_{js\text{-}As}$)

All raw image data of the tank bottom, captured in jpeg format by the camera, were transferred to a computer for further analysis. Images were converted to 8-bit images and then processed with ImageJ software 1.48 (http://imagej.nih.gov/ij/download.html) to quantify the area covered by solid particles

still at the bottom of the tank at each N. The known internal diameter of the tank was used as a scale (Figure 2.5 (a)). In the first and preliminary analysis of the first image one of the areas covered by solids at the tank bottom was manually traced, in the software, and a color threshold was assigned to this entire area (which actually contained a gradient of color shades) in order to instruct the software on how to differentiate the solids areas from the liquid background and generate a black-and-white high-contrast image (Figure 2.5). From now on, this threshold was used in all other images to identify the total area covered by solids (black) from that occupied by liquid (white) and generate a black (solids)-and-white (water) processed image. Then, in any new image, the software quantified the area, A_s, of the tank bottom covered by solids relative to the total bottom area. The value of A_s was obtained from each image. A plot of A_s vs. N was then constructed, a regression line was passed through these points, and the value of N for $A_s \rightarrow 0$ was taken as the observer-independent estimated value of N_{js}, called here $N_{js\text{-}As}$.

This same approach was also applied to the hemispherical tank, to check if the method worked for this system as well. As compared to hemispherical tank, the solids in the flat bottom tank were scattered all over the vessel bottom than in a circular fashion. Therefore, determining the area of the solid using this approach was the only option to determine N_{js} for the flat-bottomed tank.

(a) (b)

Figure 2.4 Images of tank bottom analyzed using image J: (a) Raw image of tank bottom (b) conversion into an 8-bit image

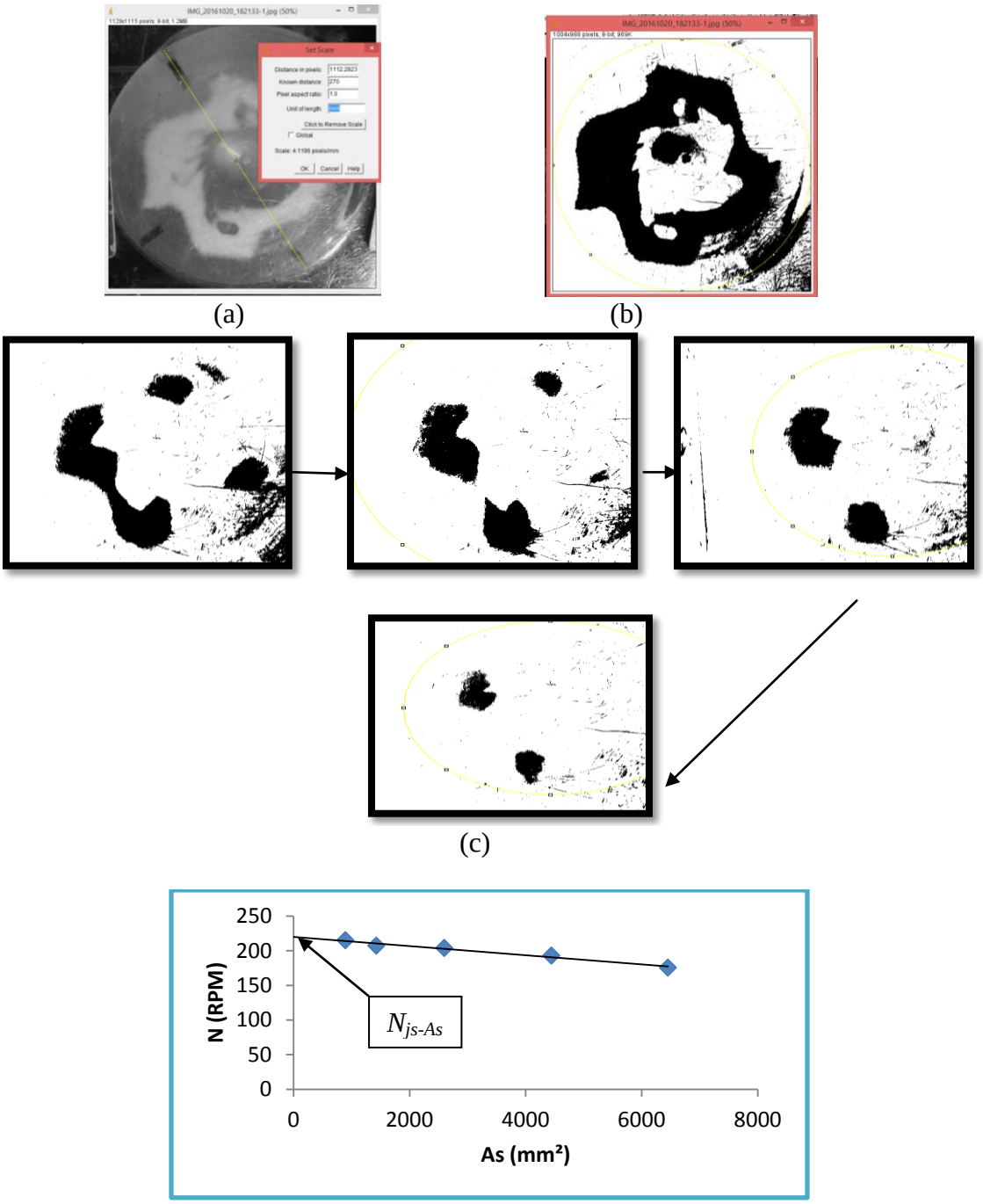

Figure 2.5 Images of tank bottom analyzed using image J: (a) set scale; (b) Thresholding of the image and analysis of the area of particles; (c) Area of solids (black) as increasing rotational speeds; (d) Graphical plot of N vs Area in order to determine $N_{js.}$

CHAPTER 3

RESULTS AND DISCUSSION

3.1 Results of Solid Suspension Experiments

3.1.1 Determination of the N_{js} Values Obtained with the Proposed Methods and Comparison of with Those Obtained with the Conventional Visual Approach in the Flat-Bottomed Tank

In this section, the results of the experiments aimed at validating the proposed method are presented and compared with results obtained by the conventional visual approach.

According to the procedure developed for the proposed method, values of A_S were obtained at increasing values of the agitation speed, N. For each experimental configuration, at least four measurements of N vs. A_S were taken. $N_{js\text{-}Visual}$ was also determined. Figures 3.1-3.5 show the N-vs.-A_S plots for different impellers and impeller clearance and the resulting $N_{js\text{-}As}$ values. These figures shows that the regression lines typically have high correlation coefficients, i.e., the points align themselves well on a straight line. In addition, these figures also report the value of the visually obtained N_{js} ($N_{js\text{-}Visual}$). In general, the values of $N_{js\text{-}As}$ and $N_{js\text{-}Visual}$ were very close to each other.

The values of N_{js} were also experimentally obtained in hemispherical-bottomed tank equipped with the Disk turbine and Pitch-blade turbine. This was a test to verify the method developed earlier. New method was then applied to both flat bottomed tank as well as hemispherical bottomed tank.

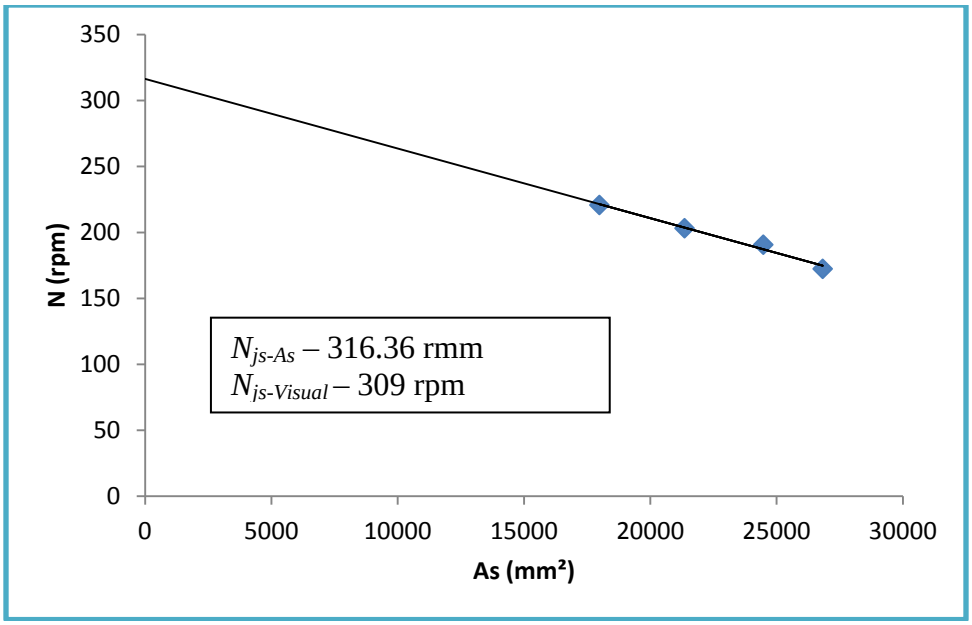

(a)

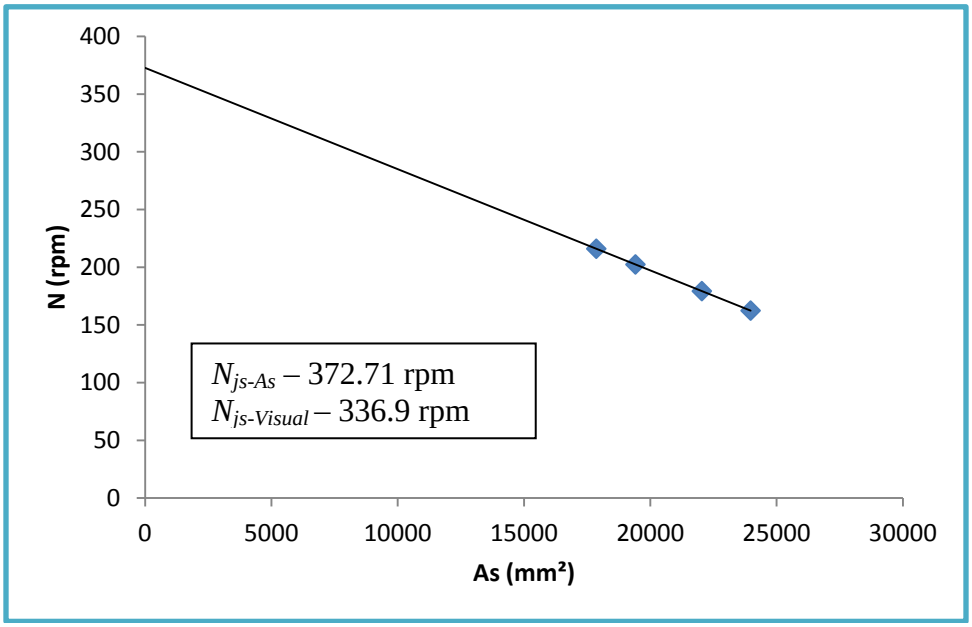

(b)

Figure 3.1 N_{js} measured the flat-bottomed tank with DT impeller for 200 µm particles at different C/T: (a) $N_{js\text{-}As}$ for C/T, 0.2 (b) $N_{js\text{-}As}$ for C/T, 0.3.

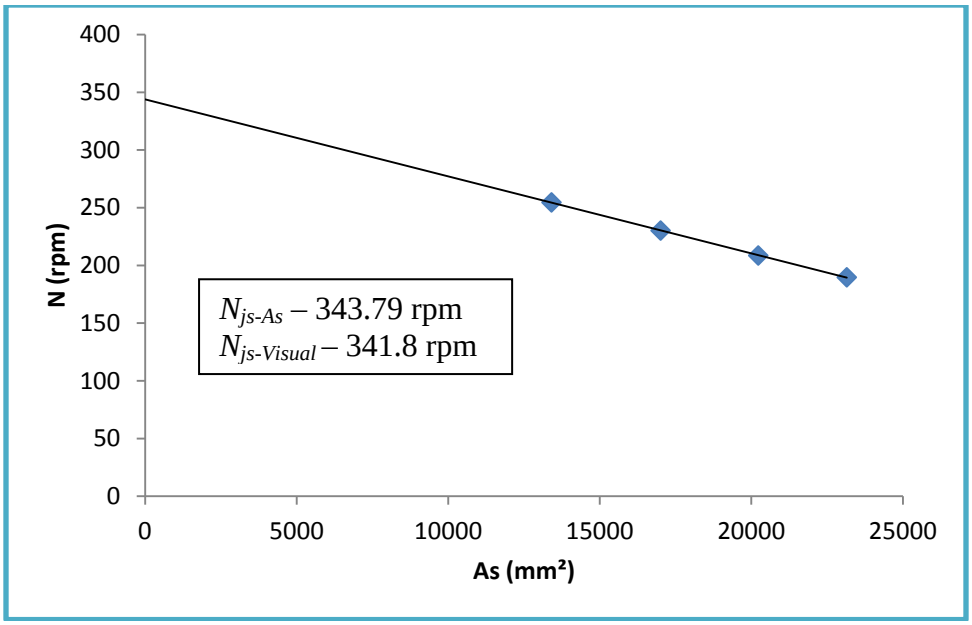

(c)

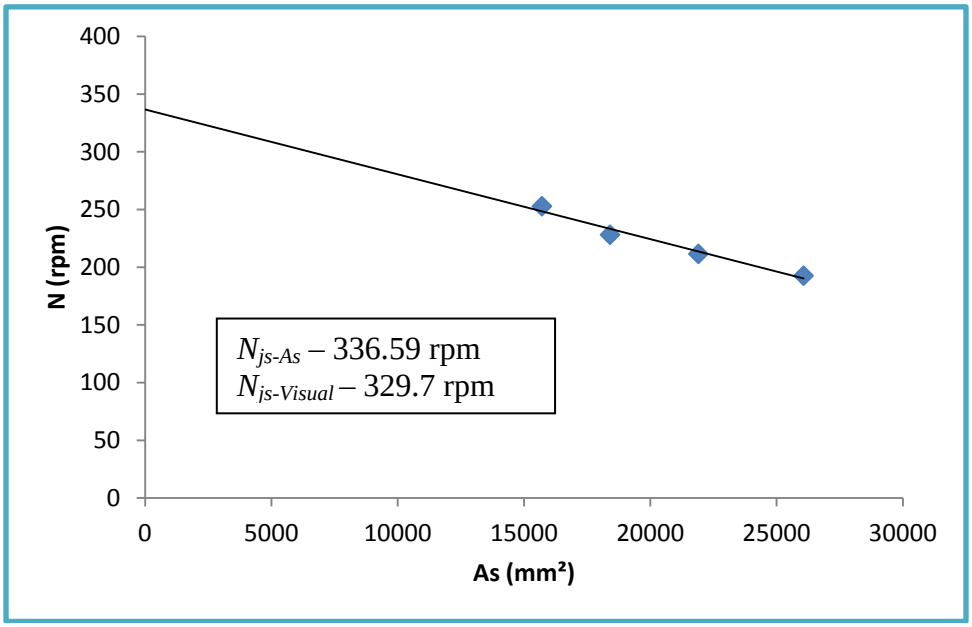

(d)

Figure 3.1 N_{js} measured the flat-bottomed tank with DT impeller for 200 µm particles at different C/T: (c) $N_{js\text{-}As}$ for C/T, 0.4; (d) $N_{js\text{-}As}$ for C/T, 0.5

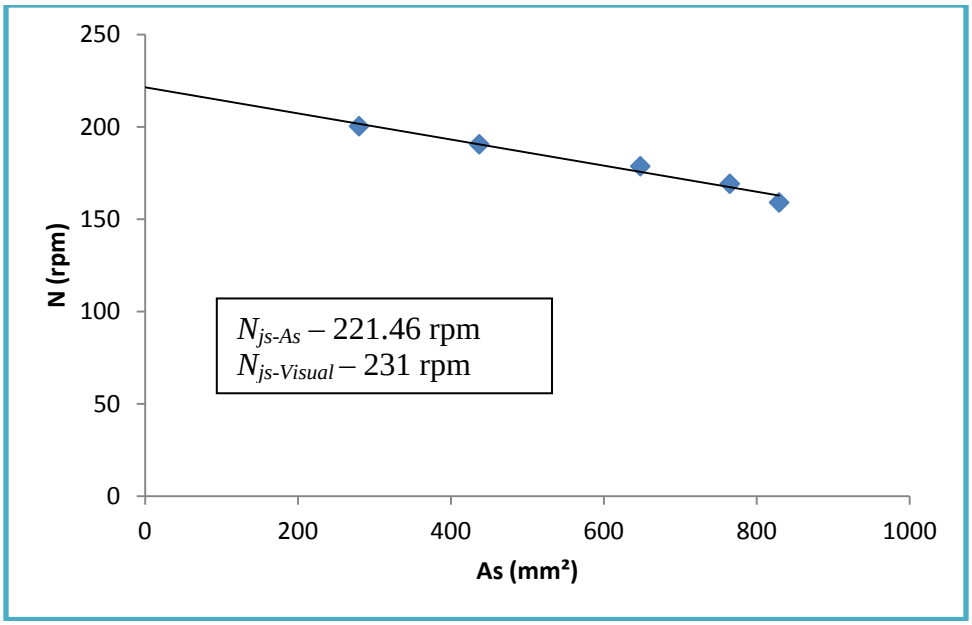

(a)

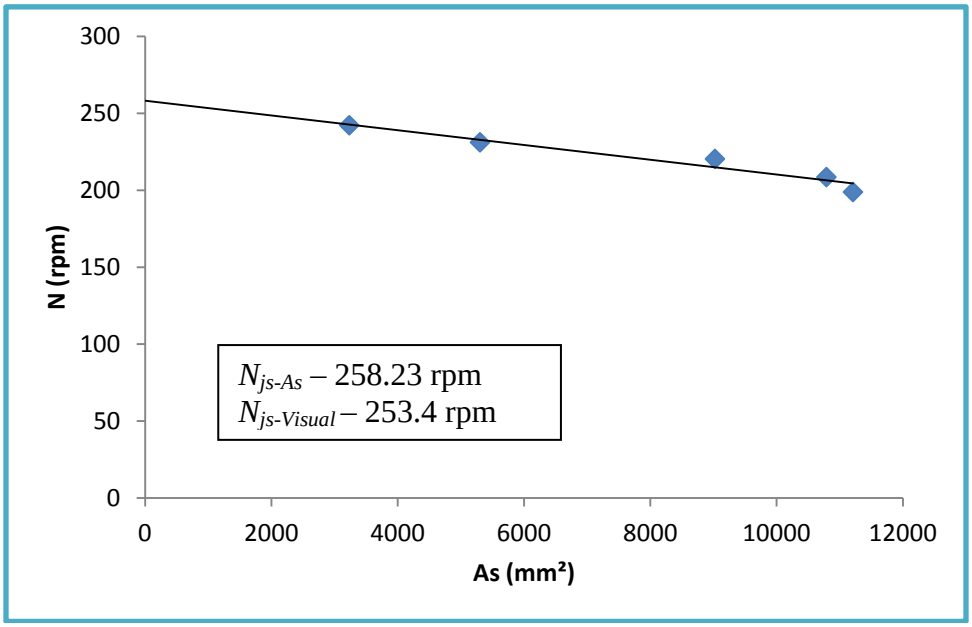

(b)

Figure 3.2 N_{js} measured the flat-bottomed tank with PBT impeller for 200 μm particles at different C/T: (a) $N_{js\text{-}As}$ for C/T, 0.2 (b) $N_{js\text{-}As}$ for C/T, 0.3.

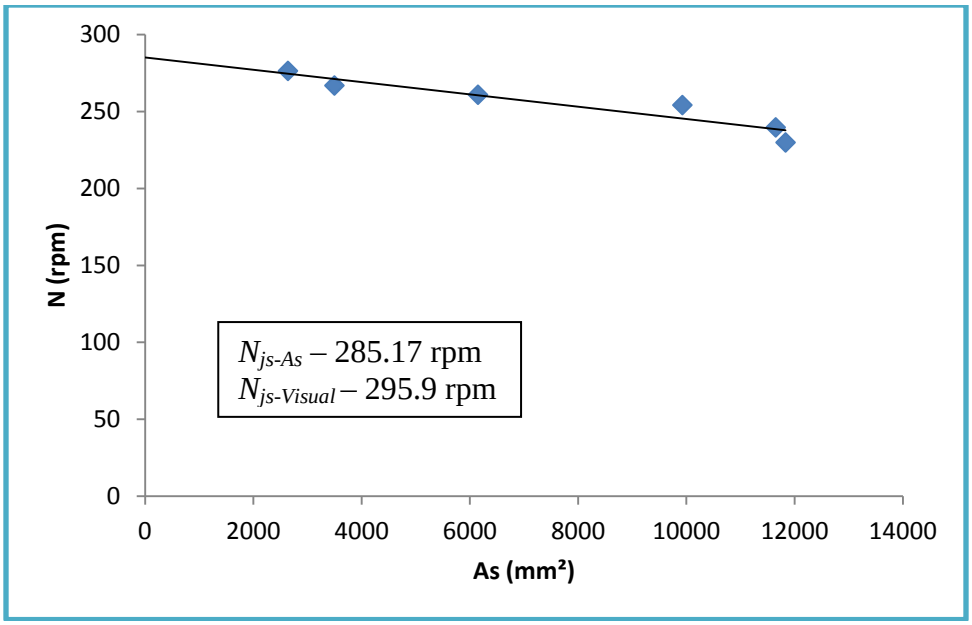

(c)

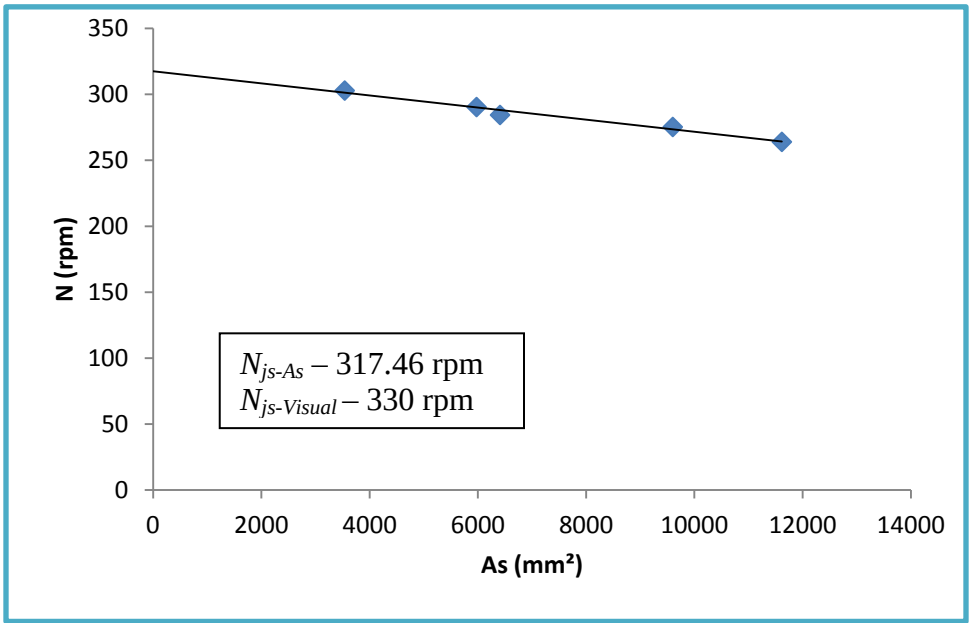

(d)

Figure 3.2 N_{js} measured the flat-bottomed tank with PBT impeller for 200 µm particles at different C/T: (c) $N_{js\text{-}As}$ for C/T, 0.4 (d) $N_{js\text{-}As}$ for C/T, 0.5

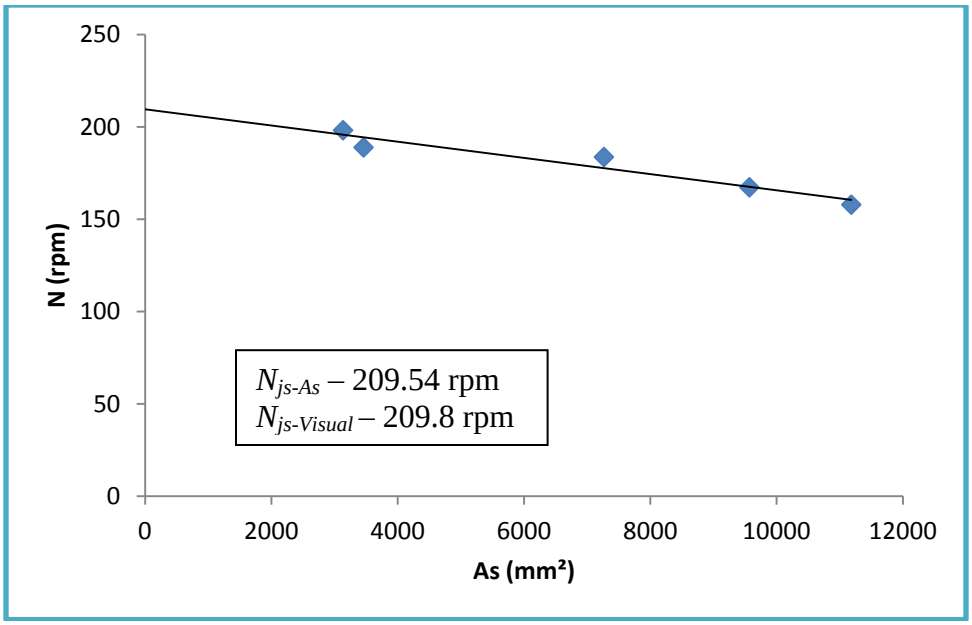

(a)

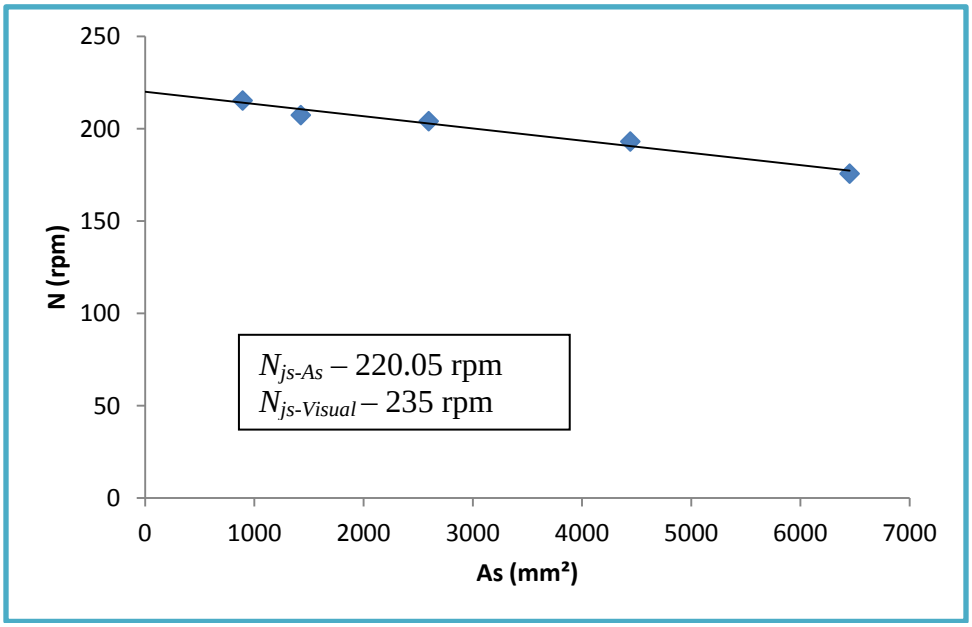

(b)

Figure 3.3 N_{js} measured the flat-bottomed tank with FBT impeller for 200 µm particles at different C/T: (a) $N_{js\text{-}As}$ for C/T, 0.2 (b) $N_{js\text{-}As}$ for C/T, 0.3.

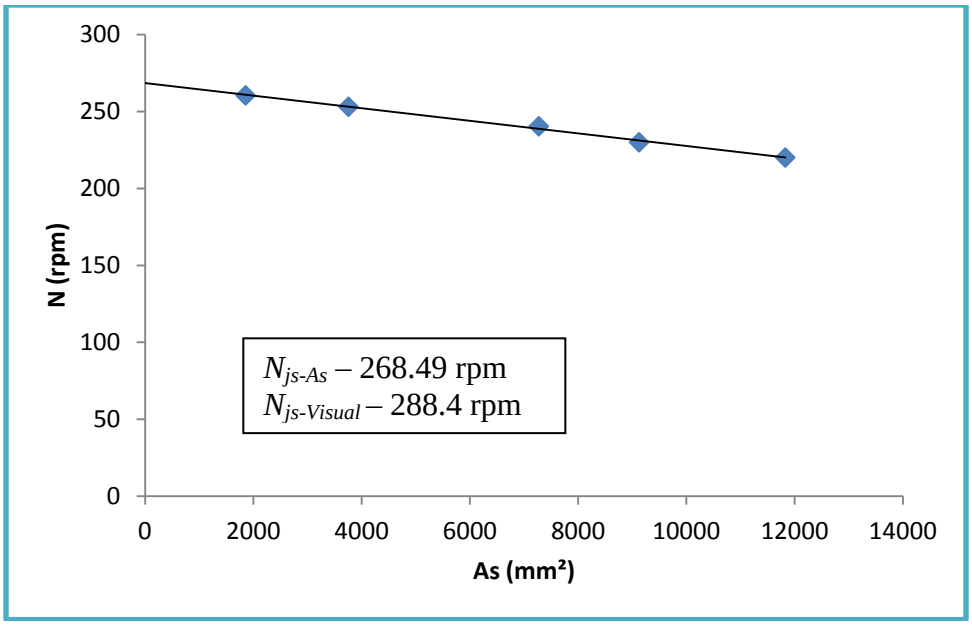

(c)

Figure 3.3 N_{js} measured the flat-bottomed tank with FBT impeller for 200 µm particles at different C/T: (c) $N_{js\text{-}As}$ for C/T, 0.4

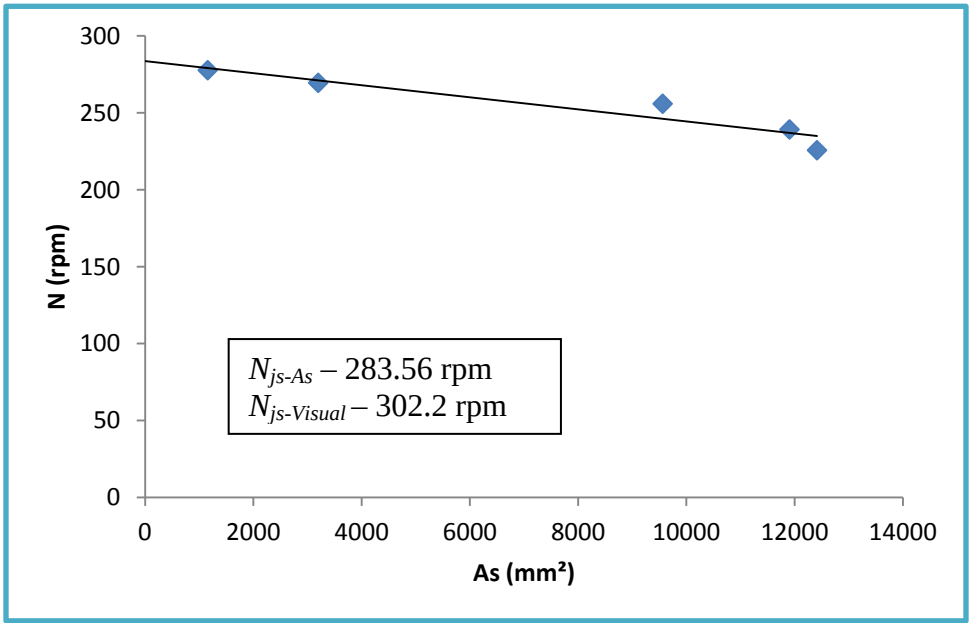

(a)

Figure 3.4 N_{js} measured the flat-bottomed tank with A310 impeller for 200 µm particles at different C/T: (a) $N_{js\text{-}As}$ for C/T, 0.2.

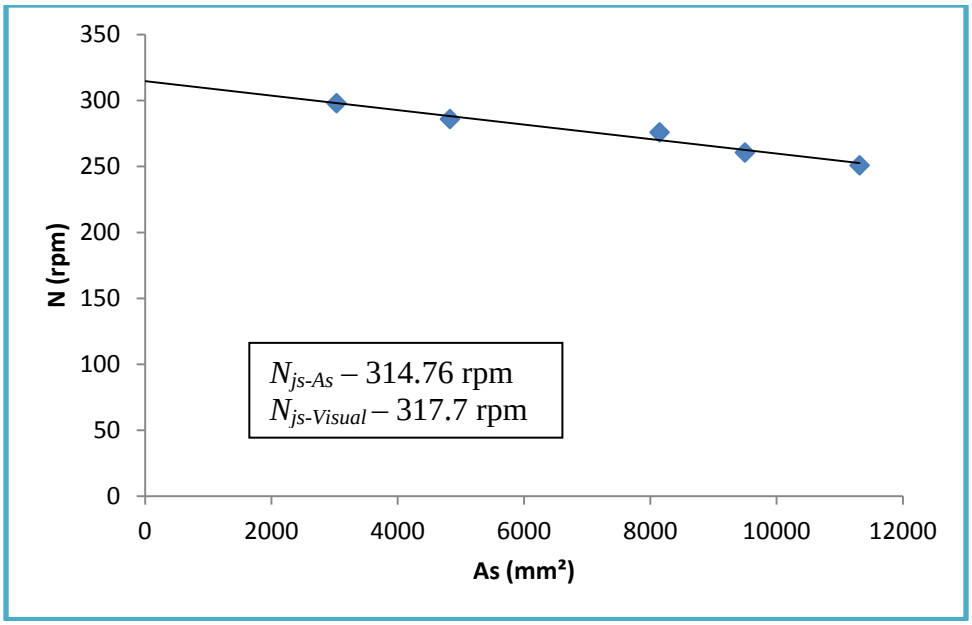

(b)

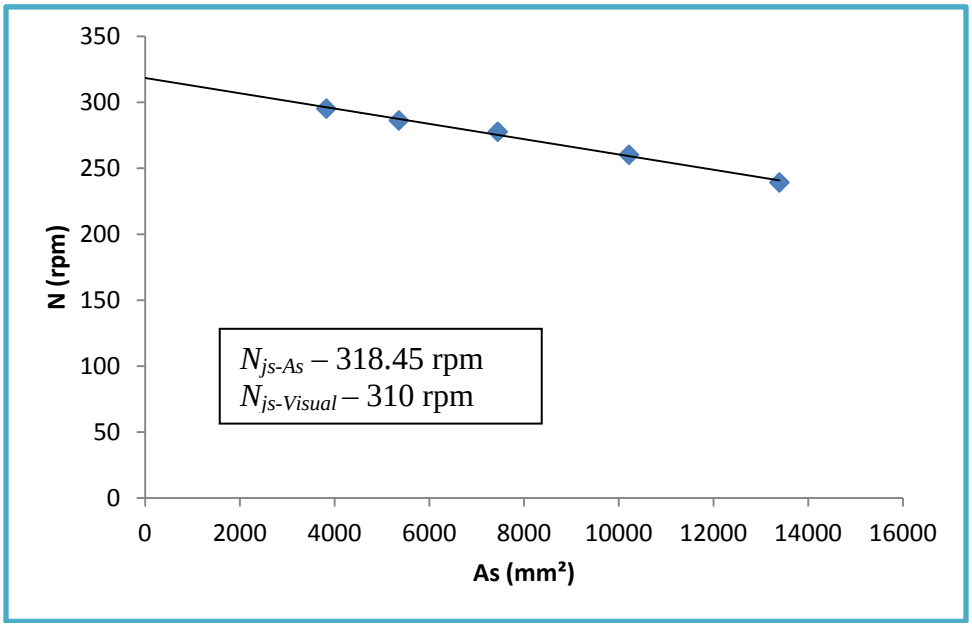

(c)

Figure 3.4 N_{js} measured the flat-bottomed tank with A310 impeller for 200 µm particles at different C/T: (b) $N_{js\text{-}As}$ for C/T, 0.25 (c) $N_{js\text{-}As}$ for C/T, 0.3

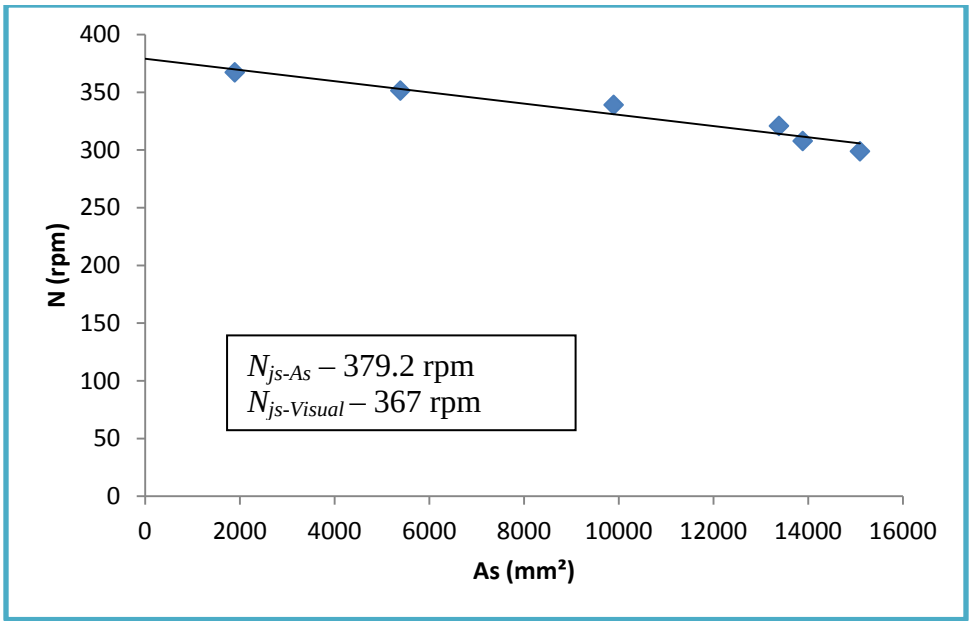

(a)

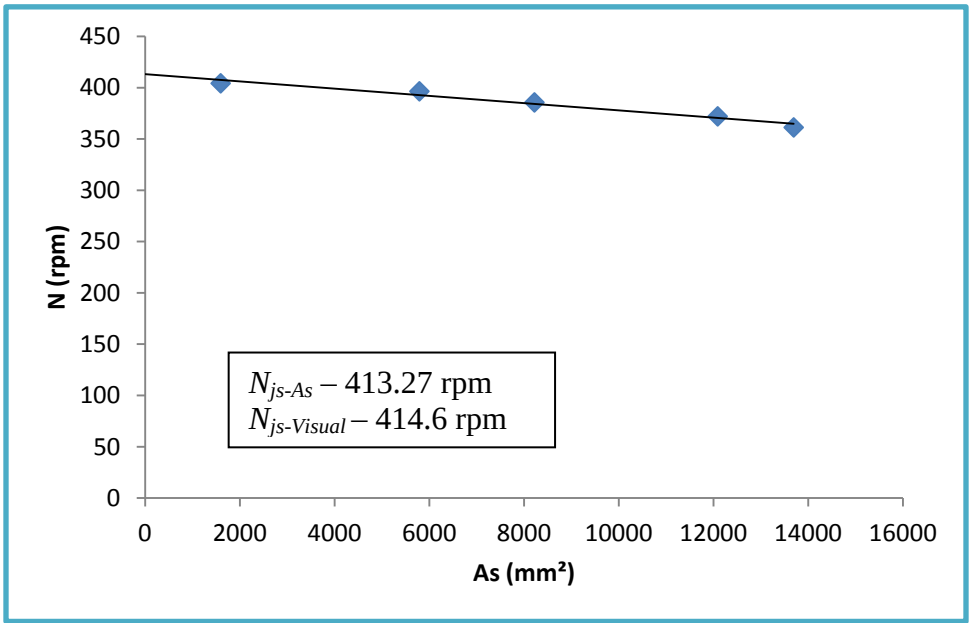

(b)

Figure 3.5 N_{js} measured the flat-bottomed tank with propeller for 200 μm particles at different C/T: (a) $N_{js\text{-}As}$ for C/T, 0.2 (b) $N_{js\text{-}As}$ for C/T, 0.25.

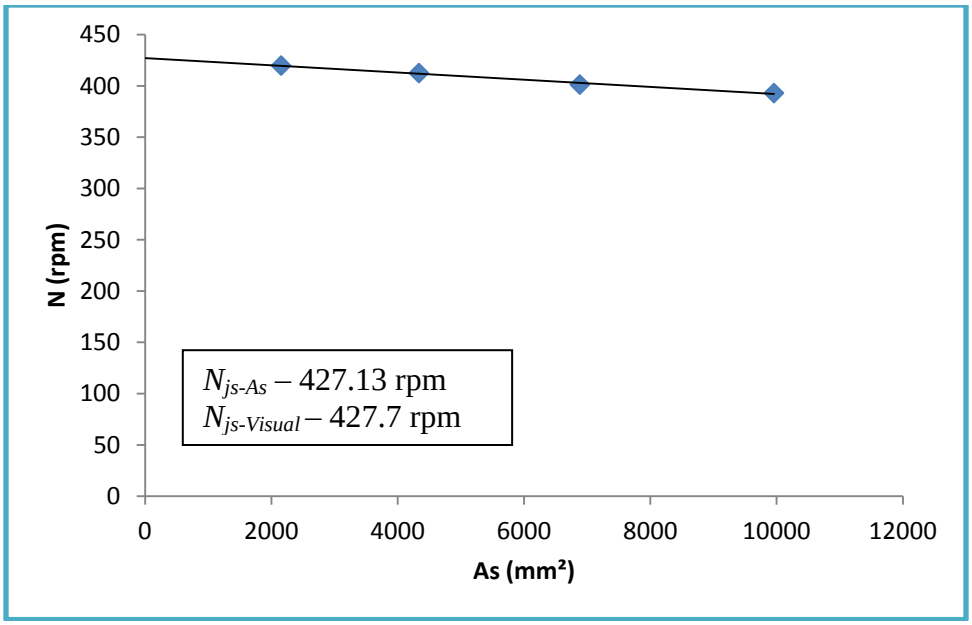

(c)

Figure 3.5 N_{js} measured the flat-bottomed tank with propeller for 200 μm particles at different C/T: (c) $N_{js\text{-}As}$ for C/T, 0.3

The results of these experiments clearly show that this novel approach for determining the N_{js} using the new method was clearly consistent for the flat-bottomed tanks as the value of N_{js} obtained using area method was in line with those obtained by visual approach.

It can be concluded that the proposed approach to N_{js} determination is valid, at least for the systems tested here, and that this method can be extended to other systems under different operating conditions, as shown below.

3.1.2 Determination of the N_{js} Values Obtained with the Proposed Methods and Comparison of with Those Obtained with the Conventional Visual Approach in the Hemispherical-Bottomed Tank

In order to compare the applicability of this method to various other systems, N_{js} of hemispherical tank was determined using this new approach.

Table 3.1 Results for $N_{js\text{-}As}$ with DT, 200 μm Particles in a hemispherical bottom reactor

Impeller type	Particle Size (μm)	Tank Diameter (mm)	Baffling	D/T	Cb/T	$N_{js\text{-}As}$ (RPM)	$N_{js\text{-}visual}$ (RPM)
DT	200	300	FB	0.33	0.35	195	200
DT	200	300	FB	0.33	0.4	180	190
DT	200	300	FB	0.33	0.45	174	183
DT	200	300	FB	0.33	0.5	170	177.5

Table 3.2 Results for $N_{js\text{-}As}$ with PBT, 200 μm Particles in a hemispherical bottom reactor

Impeller type	Particle Size (μm)	Tank Diameter (mm)	Baffling	D/T	Cb/T	$N_{js\text{-}As}$ (RPM)	$N_{js\text{-}visual}$ (RPM)
PBT	200	300	FB	0.33	0.35	272	281
PBT	200	300	FB	0.33	0.4	294	296
PBT	200	300	FB	0.33	0.45	301	298
PBT	200	300	FB	0.33	0.5	317	328

The above table shows $N_{js\text{-}As}$ for a hemispherical bottomed tank using two different impellers. The data clearly shows that the N_{js} obtained using the new method is very close to that obtained by visual observation. The solid deposited at the bottomed of the hemispherical tank typically formed circular shapes, whose area was calculated using Image J software in a relatively in a simple manner, using the approach discussed earlier.

3.1.3 N_{js} Results for Different Systems and Operation Conditions

Having preliminarily validated the newly proposed, observed-independent method to N_{js} determination, results for N_{js} were obtained for different systems under different operating conditions. The validity of this new method was evaluated using various impeller size, by varying D/T, C/T, tank size, baffling conditions, etc.

Additionally, results of N_{js} determined with 200 micrometer particles are shown in Table 3.1- Table 3.5. The Area method works well to determine N_{js} under fully baffled and partially baffled configurations. Different values of impeller diameter and tank scale up also gave results which are in acceptable limits.

Table 3.3 Results for $N_{js\text{-}As}$ with DT, 200 μm Particles

Impeller type	Particle Size (μm)	Tank Diameter (mm)	Baffling	D/T	Cb/T	$N_{js\text{-}As}$ (rpm)	$N_{js\text{-}visual}$ (rpm)
DT	200	270	FB	0.33	0.2	316	309
DT	200	270	FB	0.33	0.3	334	340
DT	200	270	FB	0.33	0.4	336	327
DT	200	270	FB	0.33	0.5	336	329
DT	200	270	FB	0.22	0.3	188	192
DT	200	270	FB	0.59	0.3	119	127
DT	200	305	UB	0.45	0.3	176	188
DT	200	305	HB	0.45	0.3	146	152
DT	200	305	FB	0.45	0.3	154	162

Table 3.4 Results for $N_{js\text{-}As}$ with PBT, 200 μm Particles

Impeller type	Particle Size (μm)	Tank Diameter (mm)	Baffling	D/T	Cb/T	$N_{js\text{-}As}$ (rpm)	$N_{js\text{-}visual}$ (rpm)
PBT	200	270	FB	0.33	0.2	221	231
PBT	200	270	FB	0.33	0.3	258	253
PBT	200	270	FB	0.33	0.4	285	295
PBT	200	270	FB	0.33	0.5	317	330
PBT	200	270	FB	0.29	0.3	345	331
PBT	200	270	UB	0.33	0.3	305	333
PBT	200	305	HB	0.33	0.3	261	283
PBT	200	305	FB	0.33	0.3	302	320

Table 3.5 Results for $N_{js\text{-}As}$ with A310, 200 μm Particles

Impeller type	Particle Size (μm)	Baffling	D/T	Cb/T	$N_{js\text{-}As}$ (rpm)	$N_{js\text{-}visual}$ (rpm)
A310	200	FB	0.45	0.2	283.56	302.2
A310	200	FB	0.45	0.3	318.45	310
A310	200	FB	0.45	0.25	314.76	317.7
A310	200	FB	0.55	0.3	239.54	225.6
A310	200	FB	0.33	0.3	387.36	383.6

Table 3.6 Results for $N_{js\text{-}As}$ with 6-FBT, 200 μm Particles

Impeller type	Particle Size (μm)	Baffling	D/T	Cb/T	$N_{js\text{-}As}$ (rpm)	$N_{js\text{-}visual}$ (rpm)
FBT	200	FB	0.33	0.2	209.54	209.8
FBT	200	FB	0.33	0.25	220.05	235
FBT	200	FB	0.33	0.3	268.49	288.4

Table 3.7 Results for $N_{js\text{-}As}$ with Propeller, 200 μm Particles

Impeller type	Particle Size (μm)	Baffling	D/T	Cb/T	$N_{js\text{-}As}$ (rpm)	$N_{js\text{-}visual}$ (rpm)
Propeller	200	FB	0.33	0.2	379.2	367
Propeller	200	FB	0.33	0.3	413.27	414.6
Propeller	200	FB	0.33	0.4	427.13	427.7

In order to better visualize these results, parity plots were generated using the visual values for $N_{js\text{-}visual}$ vs. $N_{js\text{-}As}$ those obtained with the proposed method. The results are presented in Figure 3.6. Panels (a)-(d) show the data for specific systems. The closer the points align themselves on a 45º-angle-line the better the agreement. In all cases, one can see that the values of $N_{js\text{-}visual}$ agree well with those for $N_{js\text{-}As}$ for most of the systems. The R-value is close to 1.

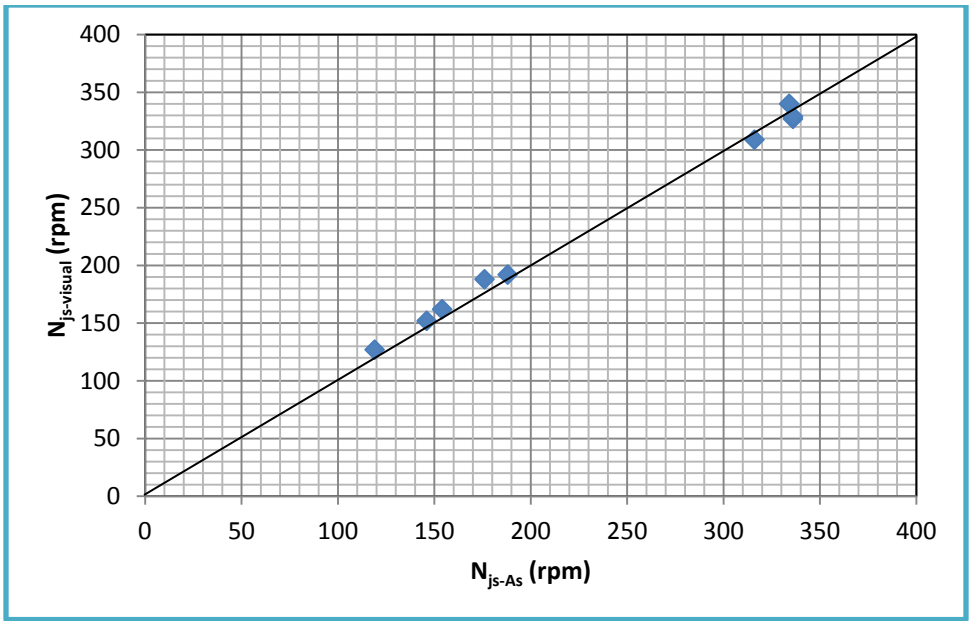

(a)

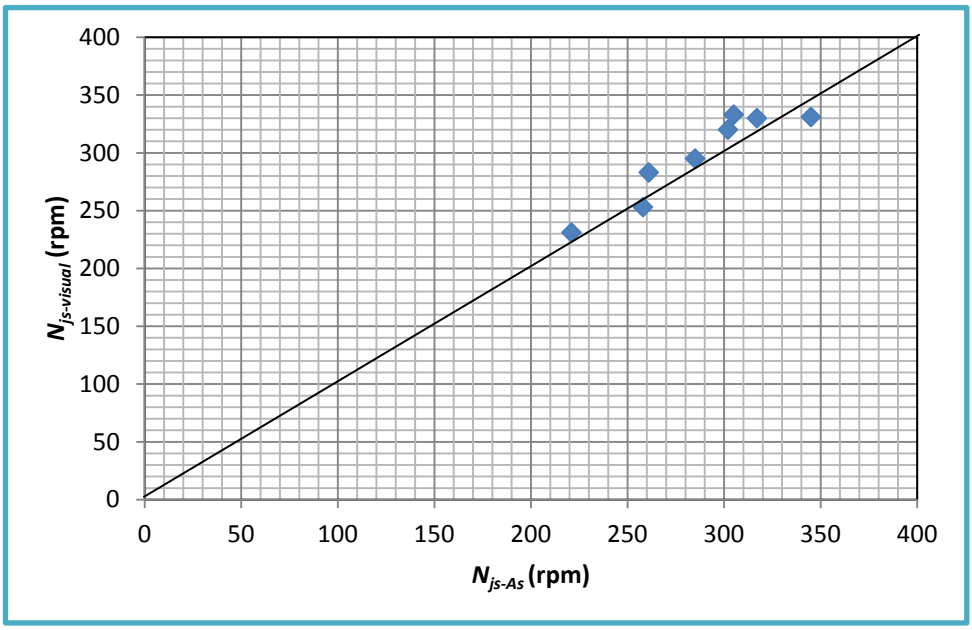

(b)

Figure 3.6 Parity plots of $N_{js\text{-}As\text{-}Method}$ (for fully baffled (FB) and partially baffled (PB) systems) and unbaffled vs. $N_{js\text{-}Visual}$. (a) Parity plot for all flat-bottomed systems with DT; (b) Parity plot for all flat-bottomed systems with PBT.

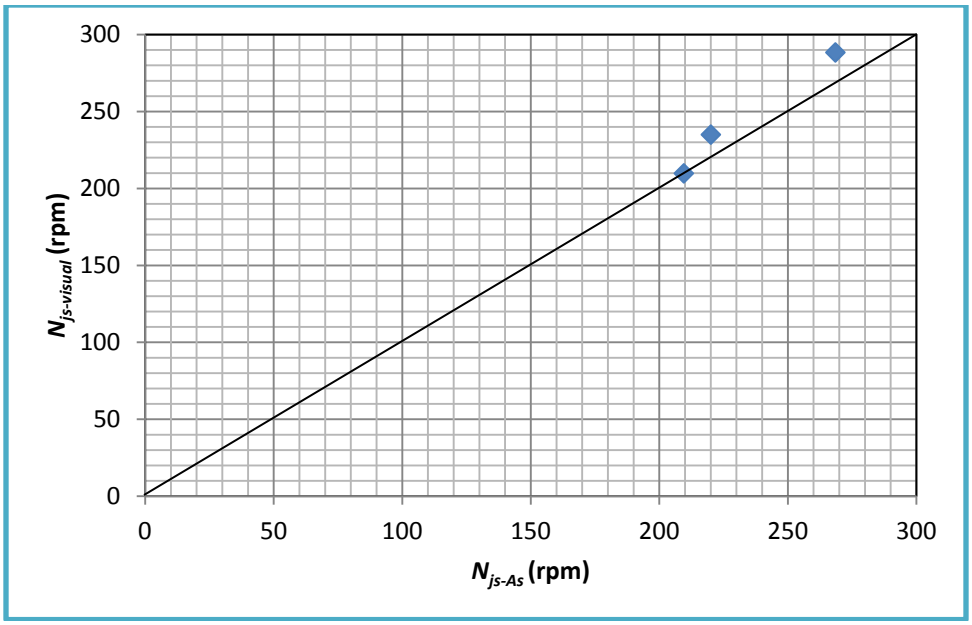

(c)

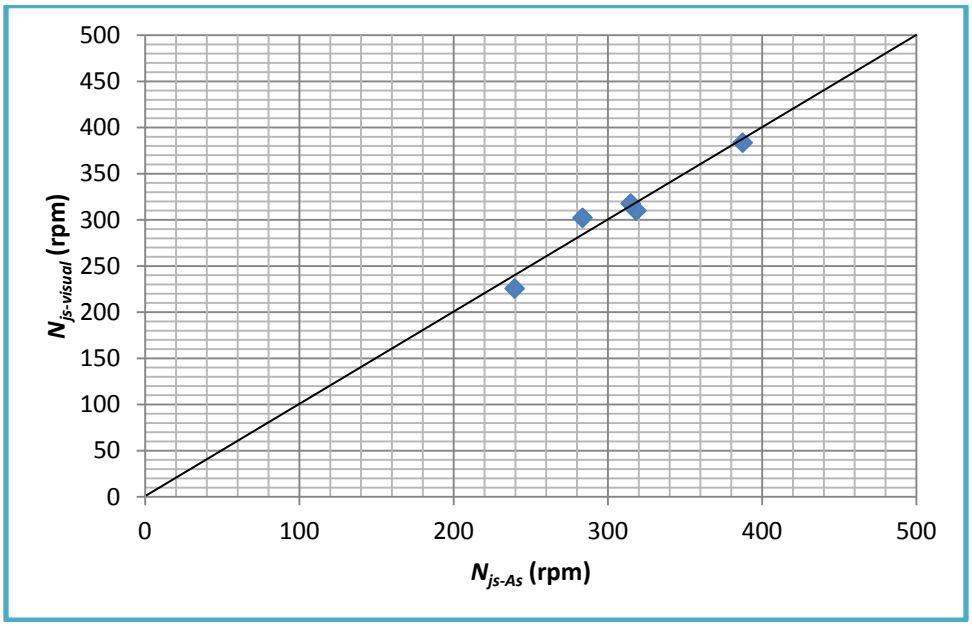

(d)

Figure 3.6 Parity plots of $N_{js\text{-}As\text{-}Method}$ (for fully baffled (FB) and partially baffled (PB) systems) and unbaffled vs. $N_{js\text{-}Visual}$. (c) Parity plot for all flat-bottomed systems with FBT (d) Parity plot for all flat-bottomed systems with A310.

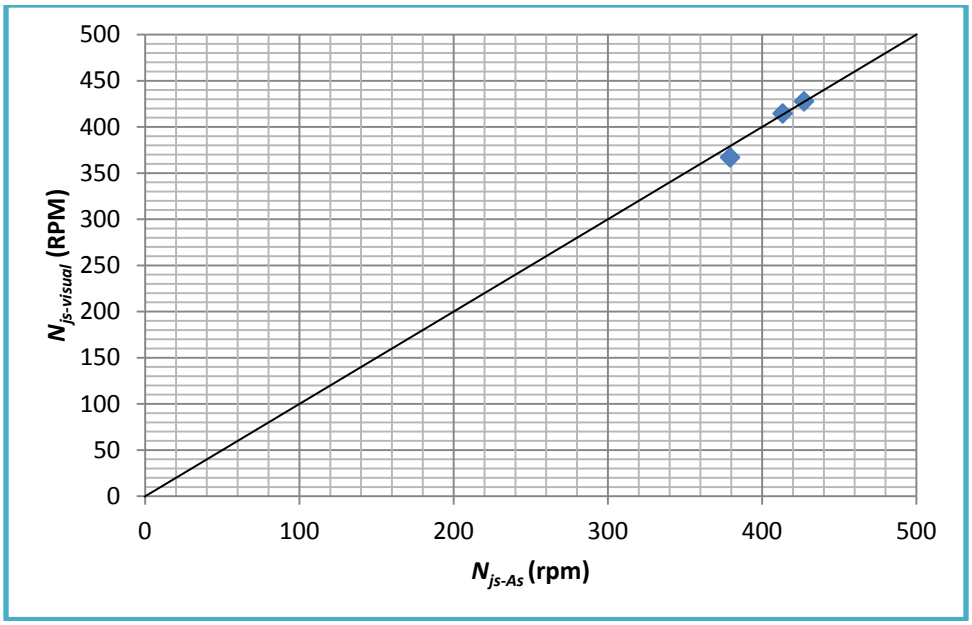

(e)

Figure 3.6 Parity plots of $N_{js\text{-}As\text{-}Method}$ (for fully baffled (FB) and partially baffled (PB) systems) and unbaffled vs. $N_{js\text{-}Visual}$. (e) parity plot for all flat-bottomed systems with Propeller.

Table 3.8 Results of Reproducibility Study

Impeller type	Particle Size (µm)	Tank Diameter (mm)	Baffling	D/T	Cb/T	$N_{js\text{-}As}$ (rpm)	$N_{js\text{-}As}$ (rpm)	$N_{js\text{-}As}$ (rpm)
						Experiment 1	Experiment 2	Experiment 3
DT	200	270	FB	0.33	0.2	316	312	320
DT	200	270	FB	0.33	0.3	334	339	337
DT	200	270	FB	0.33	0.4	336	343	348
DT	200	270	FB	0.33	0.5	336	336.55	338
PBT	200	270	FB	0.33	0.2	221	227	231
PBT	200	270	FB	0.33	0.3	258	248	252
PBT	200	270	FB	0.33	0.4	285	301	293
PBT	200	270	FB	0.33	0.5	317	319	308

In order to the reproducibility of the method identical experiments were conducted in triplicates. The results are shown in Table 3.8. This table shows the value of $N_{js\text{-}As}$ when the experiments were repeated under the same conditions and criteria. It was seen that the value of $N_{js\text{-}As}$ in with 4.7% error limit which is a clear indication of its reproducibility.

3.1.4 Comparison of the Effect of the Impeller Off-bottomed Clearance Ratio C_b/T on the Minimum Agitation Speed for Solid Suspension N_{js} for Different Mixing Systems

The values of N_{js} were experimentally obtained for different C_b/T ratios for all five systems (flat-bottomed tank with DT impeller system, flat-bottomed tank with 6-PBT, flat-bottomed tank with 6-FBT, flat-bottomed tank with A310 and flat-bottomed tank with Propeller). The results with the 200 µm particles as dispersed phase are shown in Figure 3.7(a) - 3.7(e), respectively. Triplicates experiment were conducted with all the impellers and the standard deviation of triplicate data was calculated for each point. The typical standard deviation was too small (<1%) to be plotted, indicating that the results were highly reproducible.

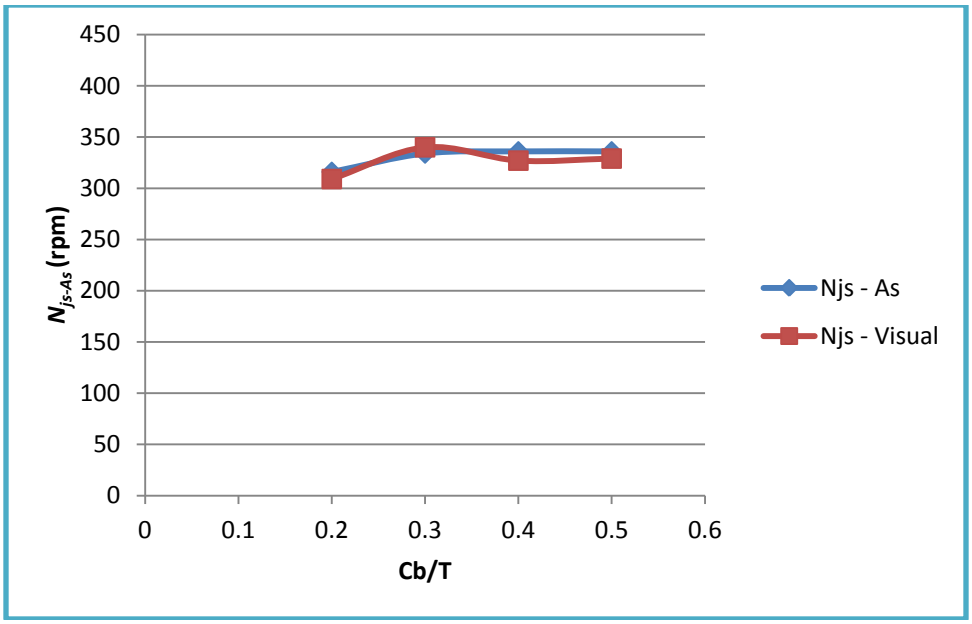

(a)

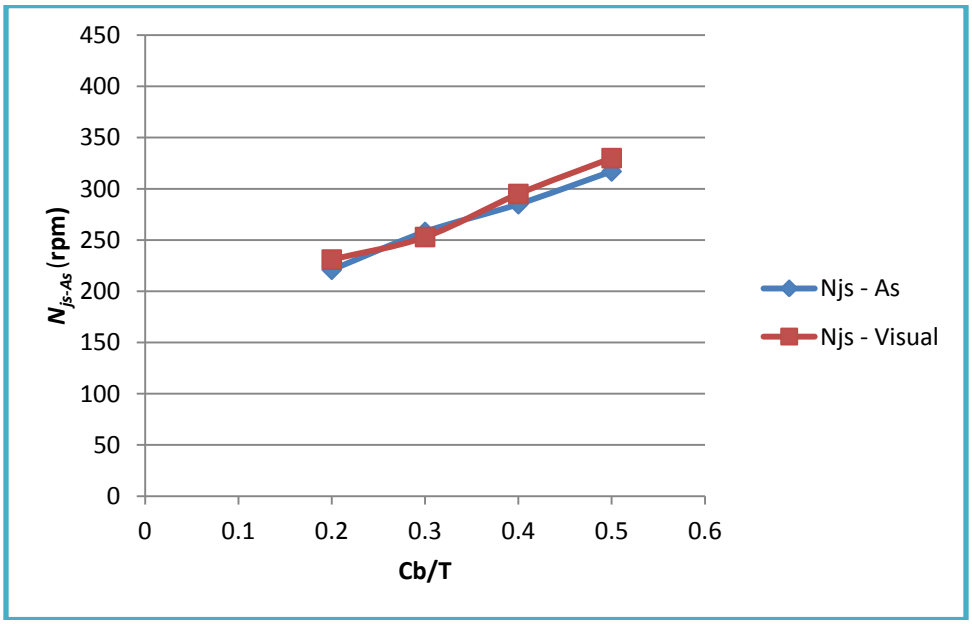

(b)

Figure 3.7 Effect of the Impeller Off-bottomed Clearance Ratio C_b/T on N_{js} for different impellers: (a) DT (200 µm Particles) (b) PBT (200µm Particles).

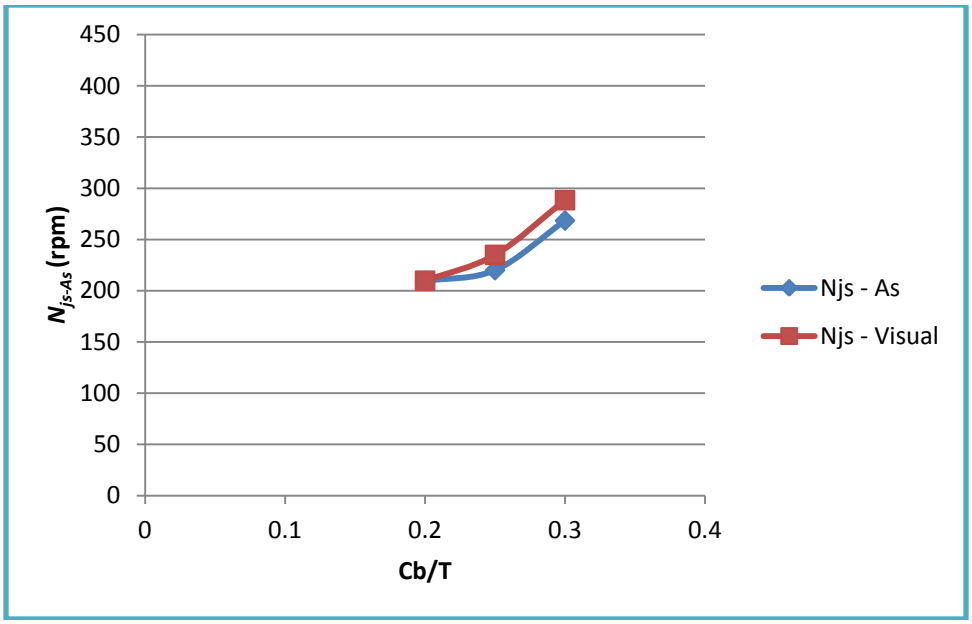

(c)

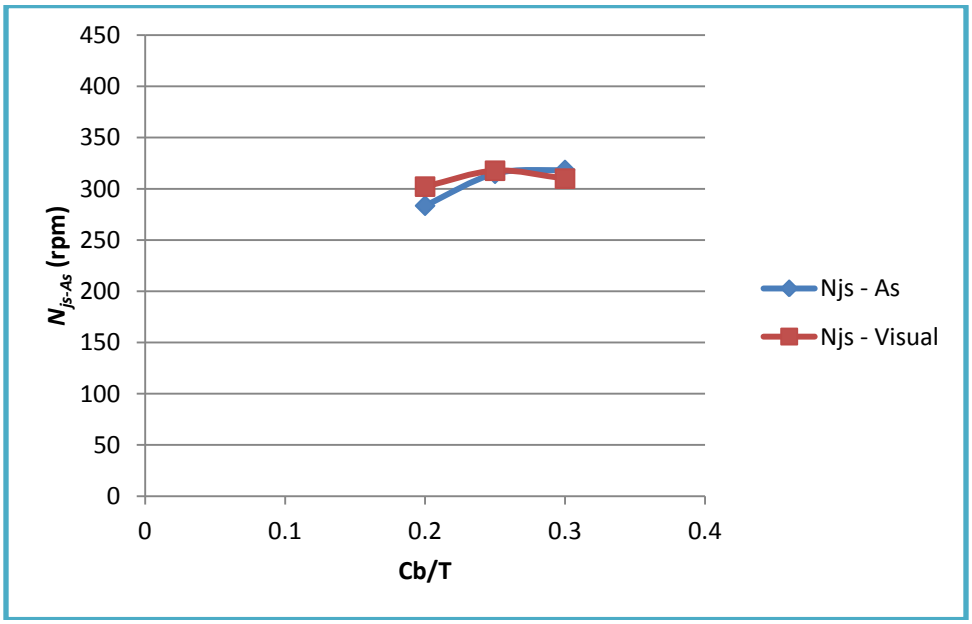

(d)

Figure 3.7 Effect of the Impeller Off-bottomed Clearance Ratio C_b/T on N_{js} for different impellers: (c) FBT (200 µm Particles); (d) A310 (200 µm Particles).

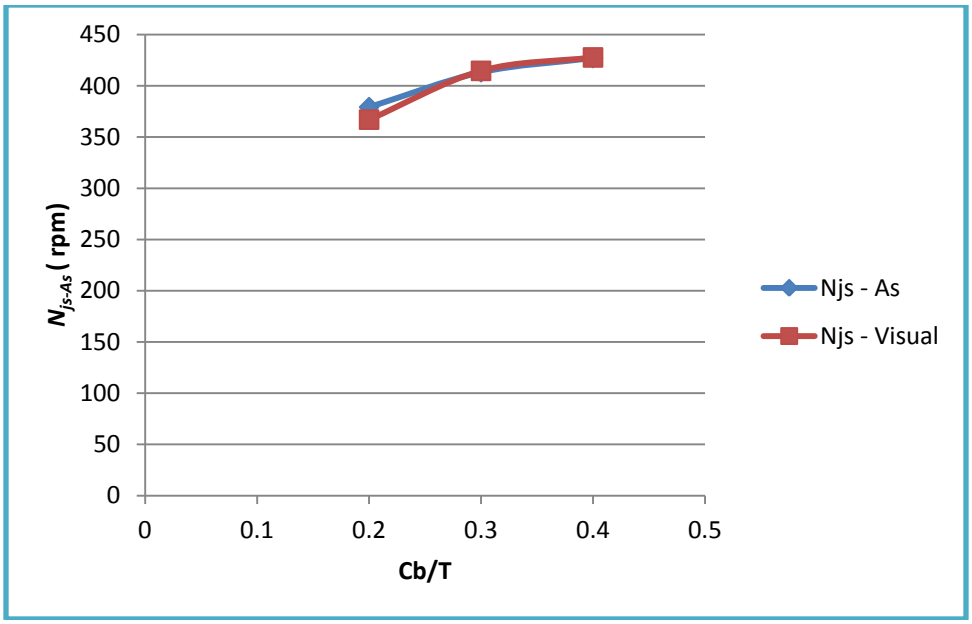

(e)

Figure 3.7 Effect of the Impeller Off-bottomed Clearance Ratio C_b/T on N_{js} for different impellers: (e) Propeller (200 µm Particles).

For all impellers, N_{js} increased with increase in impeller height from the bottomed of the tank. Only in case of DT and A310 there is a little irregularity, which may be due to some error or because of the mixing variations with change in height. Usually the increase in N_{js} is significant from 0.2 to 0.3, it is somewhat constant for value greater than 0.3.

3.1.5 Effect of the *D/T* Ratio on N_{js}

The value of N_{js} was compared by varying the size of the impeller. In case of DT, N_{js} when D/T is 0.22 was lower compared to the N_{js} when D/T is 0.33, but the N_{js} was lower when the impeller size was much bigger, that is D/T equal to 0.59. In case of PBT and A310 there was a decrease in the N_{js} with increase in impeller size. Figure 3.8 shows the variation of N_{js} at different impeller sizes.

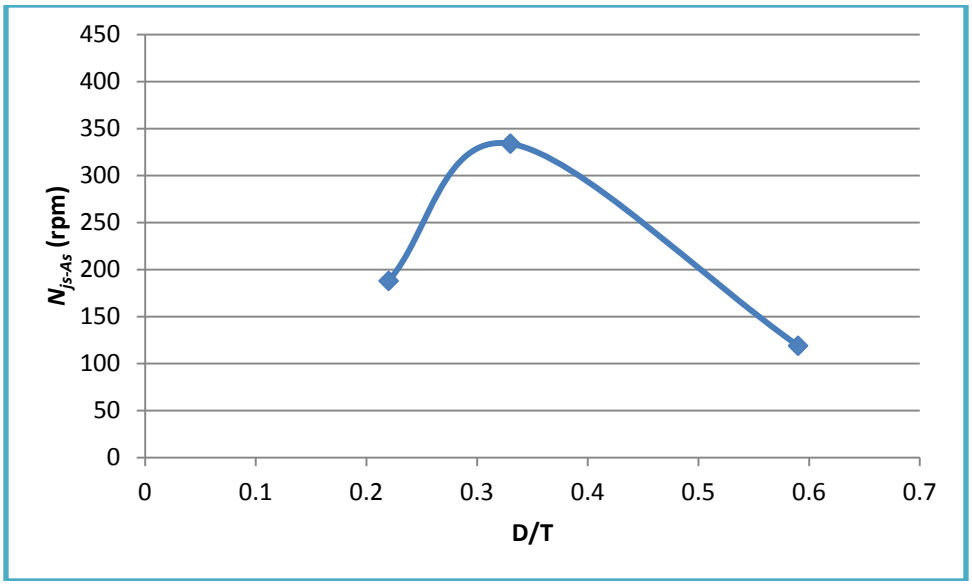

(a)

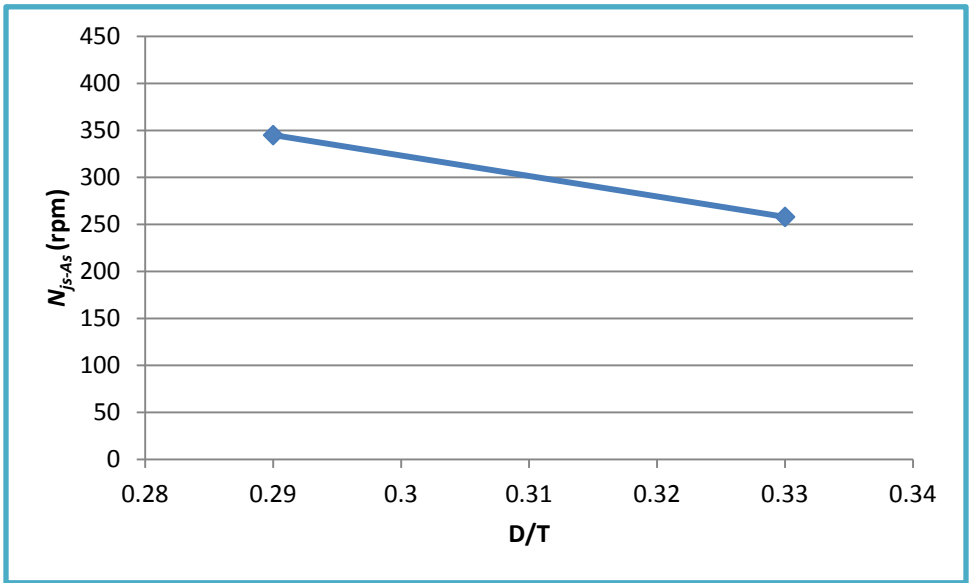

(b)

Figure 3.8 Effect of the Impeller size Ratio *D/T* on N_{js} for different Impellers: DT (200 µm Particles) (b) PBT (200µm Particles).

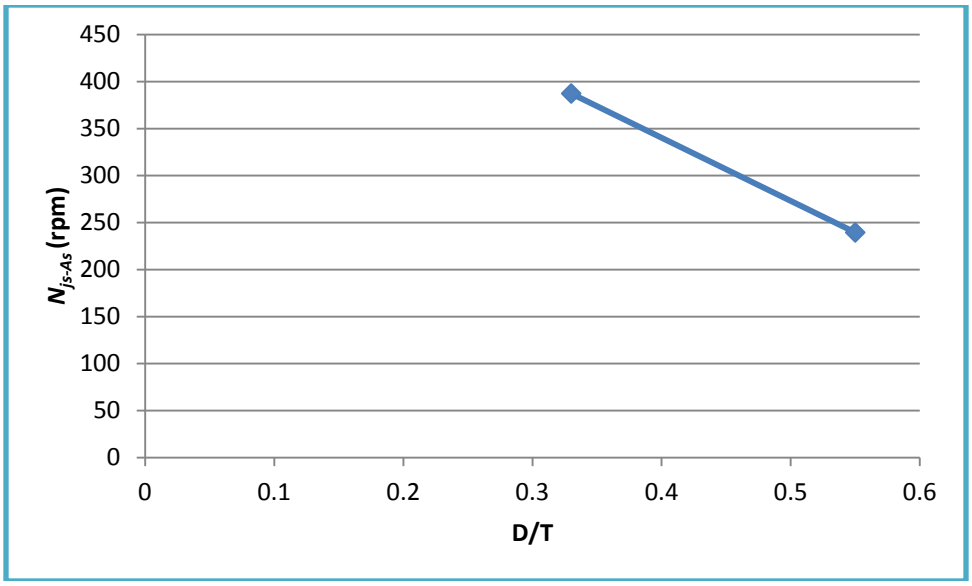

(c)

Figure 3.8 Effect of the Impeller size Ratio *D/T* on N_{js} for different Impellers: (c) A310 (200 µm Particles).

3.1.6 Effect of Particle Size on N_{js}

When the particle size was decreased it was observed that the N_{js} was relatively smaller. The size of particle was reduced from 200 µm to 150 µm. Figure 3.9 clearly gives the N_{js} for particles of 150 µm size, using 2 types of impellers, DT and PBT. In both the cases the N_{js} was observed to decrease, it took less time to suspend smaller particles. The graphs clearly shows that the new method is applicable for solid particles of any size.

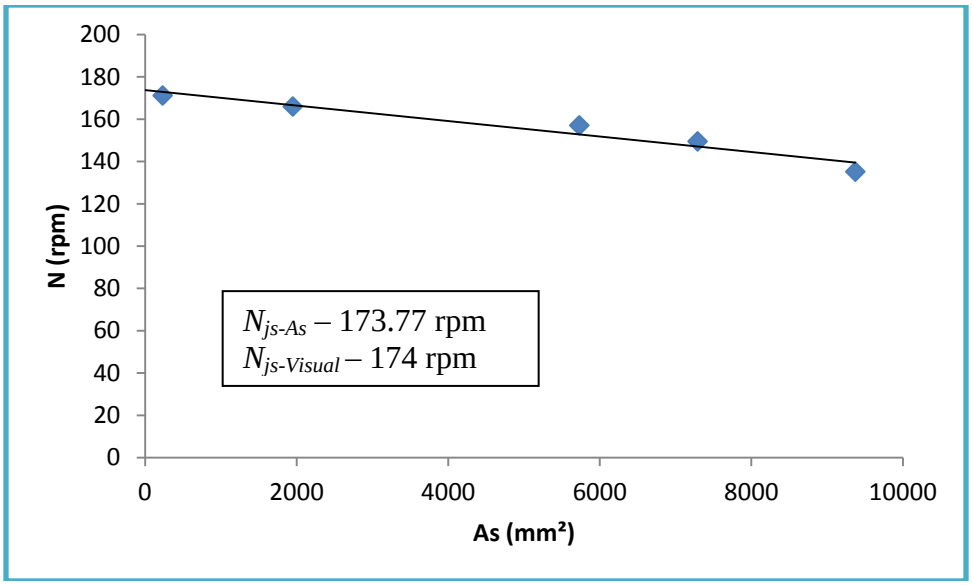

(a)

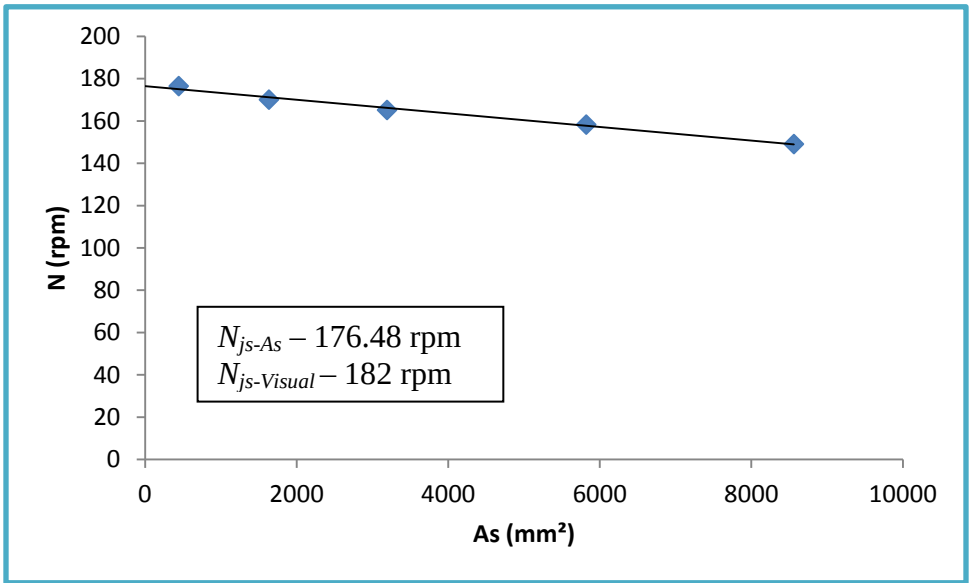

(b)

Figure 3.9 Effect of the Particle size on N_{js} for different impellers at varying *Cb/T* ratio: (a) DT (150 µm Particles), *Cb/T*-0.2; (b) DT (150 µm Particles), *Cb/T*-0.3.

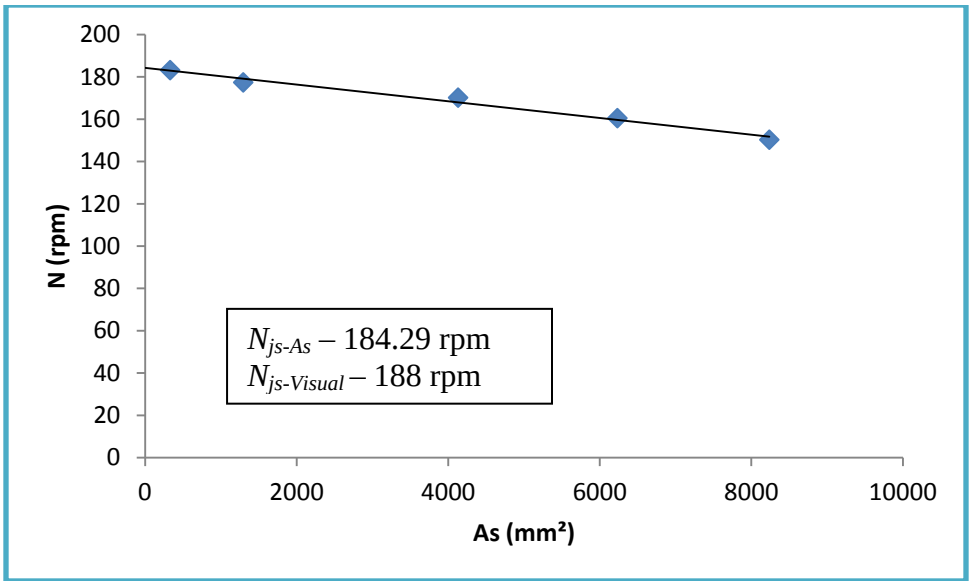

(c)

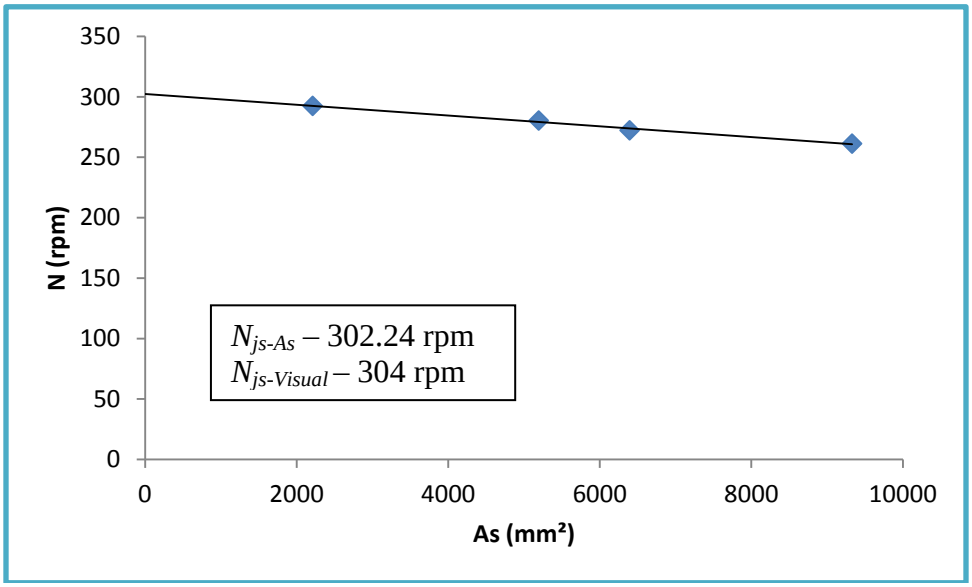

(d)

Figure 3.9 Effect of the Particle size on N_{js} for different impellers at varying *Cb/T* ratio: (c) DT (150 µm Particles), *Cb/T*-0.4; (d) PBT (150 µm Particles), *Cb/T*-0.2.

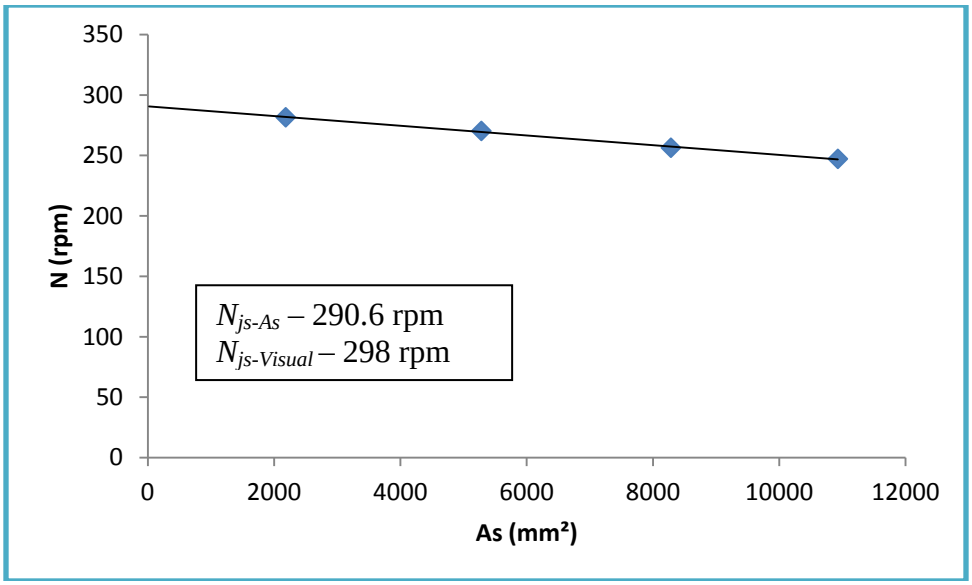

(e)

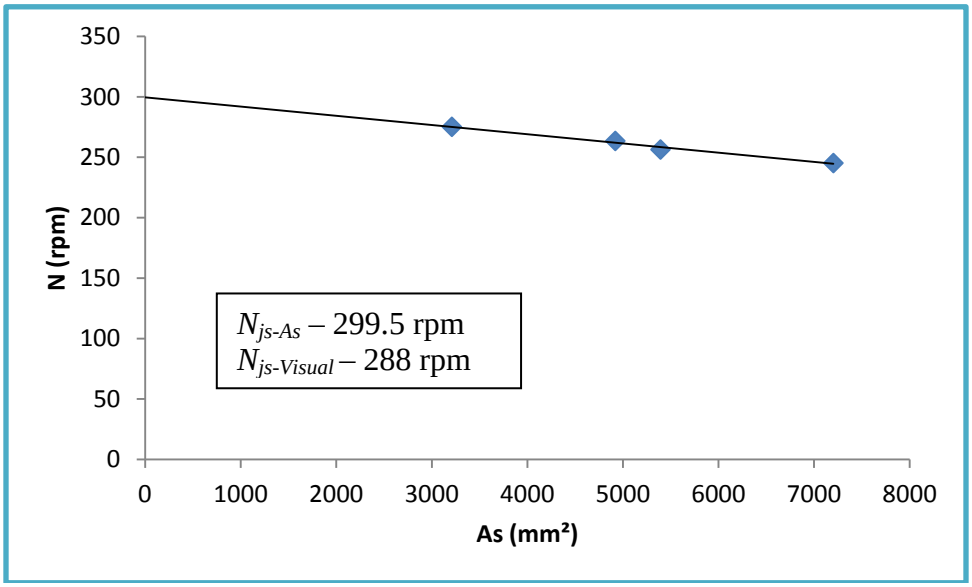

(f)

Figure 3.9 Effect of the Particle size on N_{js} for different impellers at varying *Cb/T* ratio: (e) PBT (150 µm Particles), *Cb/T*-0.3 and (f) PBT (150 µm Particles), *Cb/T*-0.4.

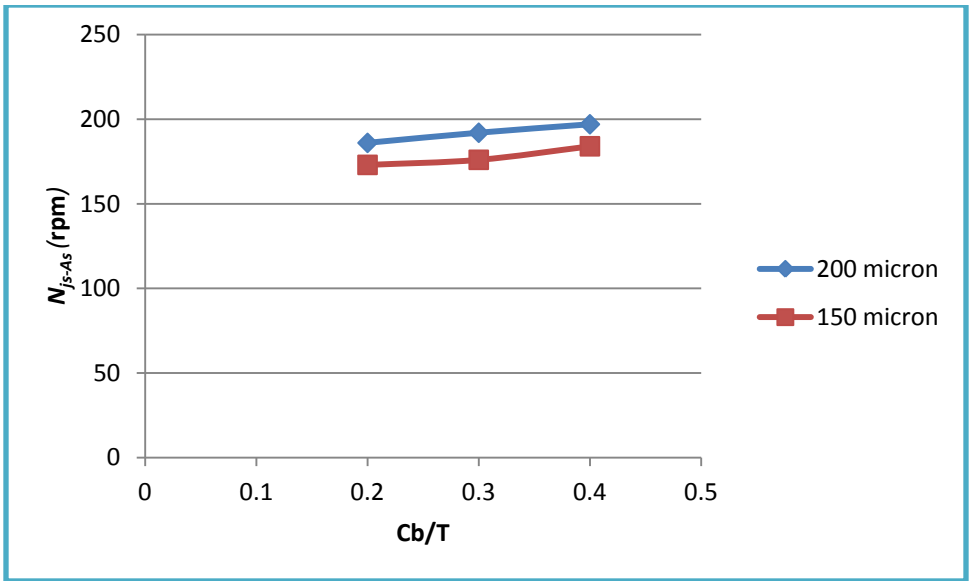

(g)

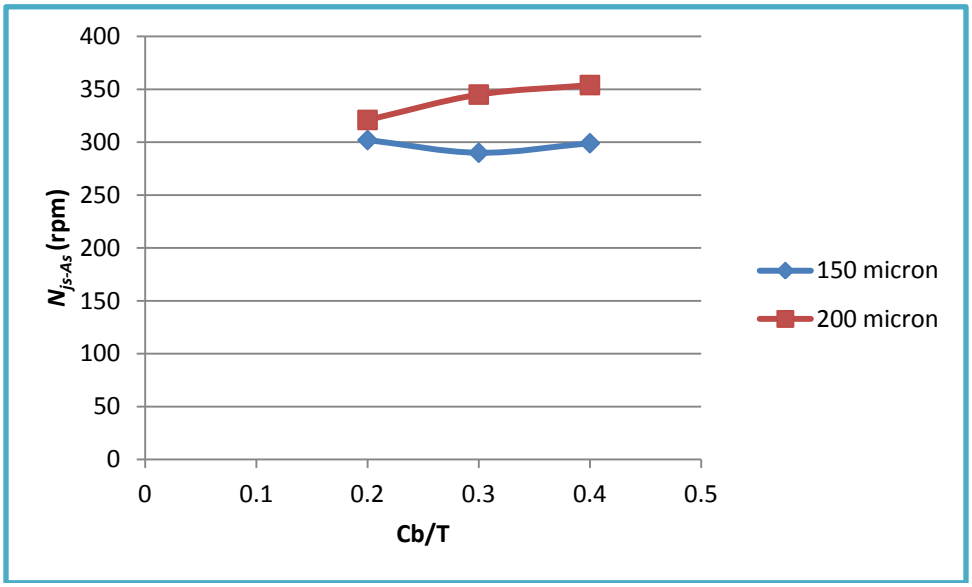

(h)

Figure 3.9 Effect of the Particle size on N_{js} for different impellers at varying *Cb/T* ratio: (g) DT comparison graph between 200 micron and 150 micron particles, for D/T ratio of 0.22; (h) DT comparison graph between 200 micron and 150 micron particles, for D/T ratio of 0.29.

3.1.7 Effect of Particle Concentration on N_{js}

Particle concentration was increased from the usual 0.5% to 0.75%. The N_{js} was comparatively higher. Observation was similar for both the impellers (DT and PBT). Figure 3.10 shows the N_{js} for different cases and criteria's in two different impellers. Time taken to suspend was higher due to increase in the amount of solids, also the change in N_{js} was not very high, only a minimal change was observed. Though the amount of solid increased the mixing pattern by the impeller was similar and thus not a lot of difference could be seen in this variability study.

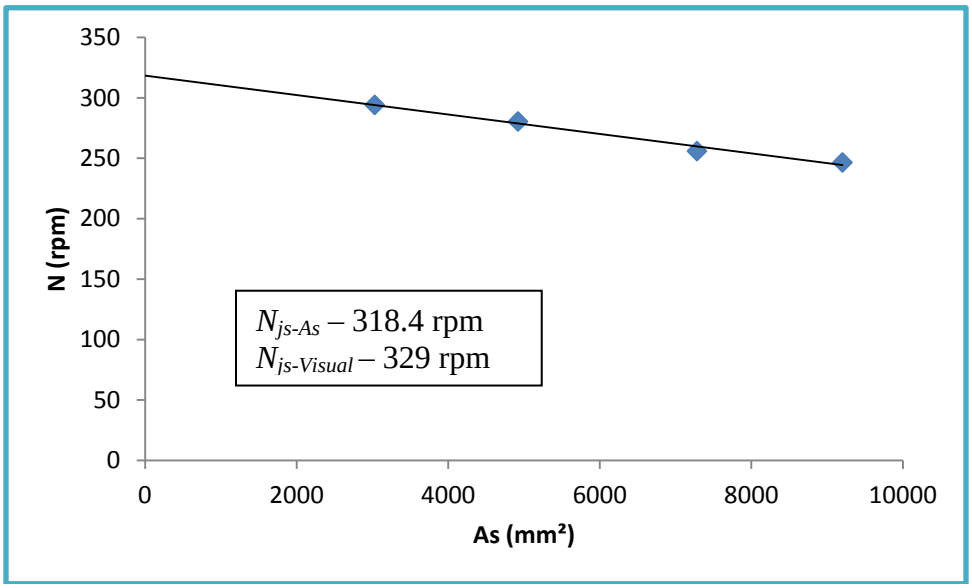

(a)

Figure 3.10 Effect of the Particle concentration on N_{js} for different impellers at varying *Cb/T* ratio: (a) DT (150 µm Particles).

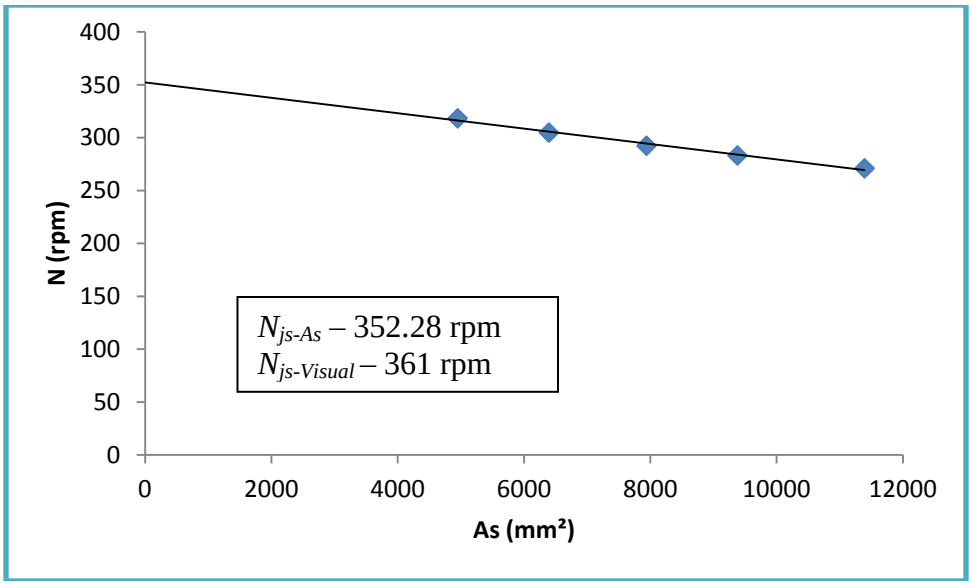

(b)

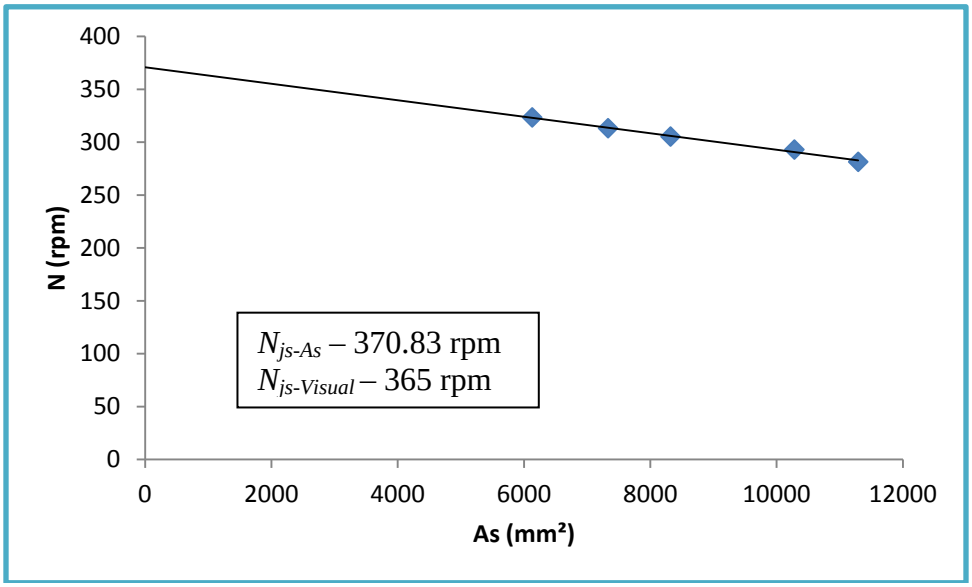

(c)

Figure 3.10 Effect of the Particle concentration on N_{js} for different impellers at varying *Cb/T* ratio: (b) DT (150 µm Particles), *Cb/T*-0.3; (c) DT (150 µm Particles), *Cb/T*-0.4.

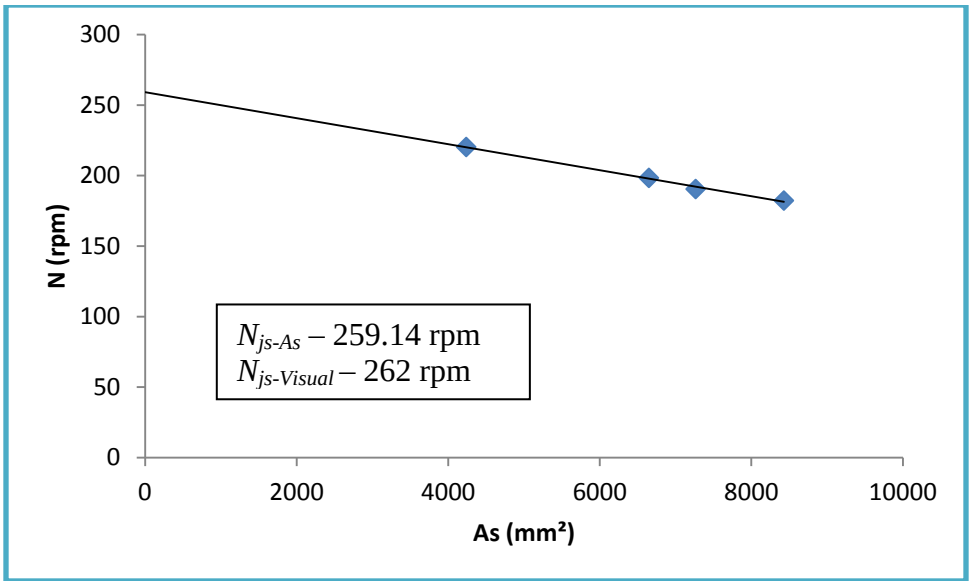

(d)

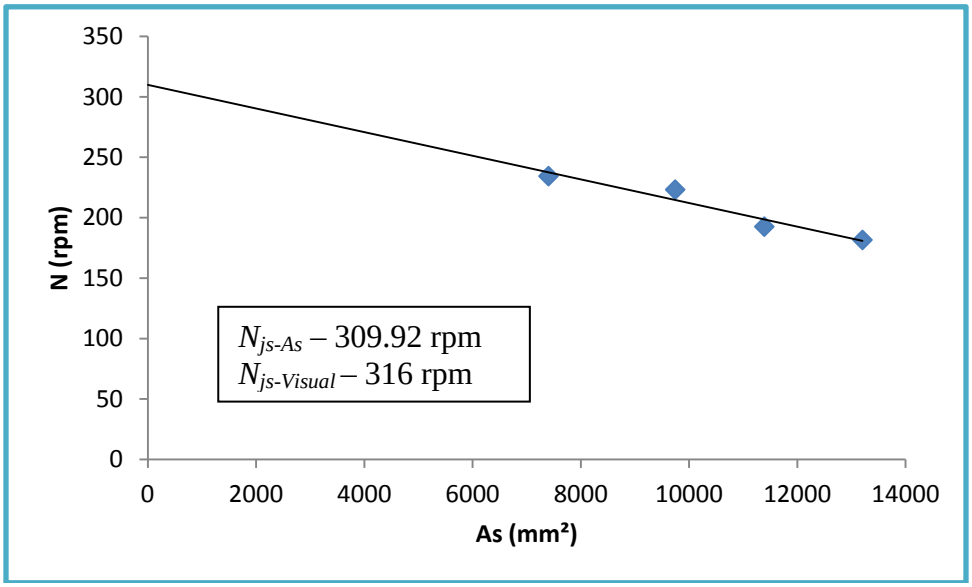

(e)

Figure 3.10 Effect of the Particle concentration on N_{js} for different impellers at varying *Cb/T* ratio: (d) PBT (150 µm Particles), *Cb/T*-0.2; (e) PBT (150 µm Particles), *Cb/T*-0.3.

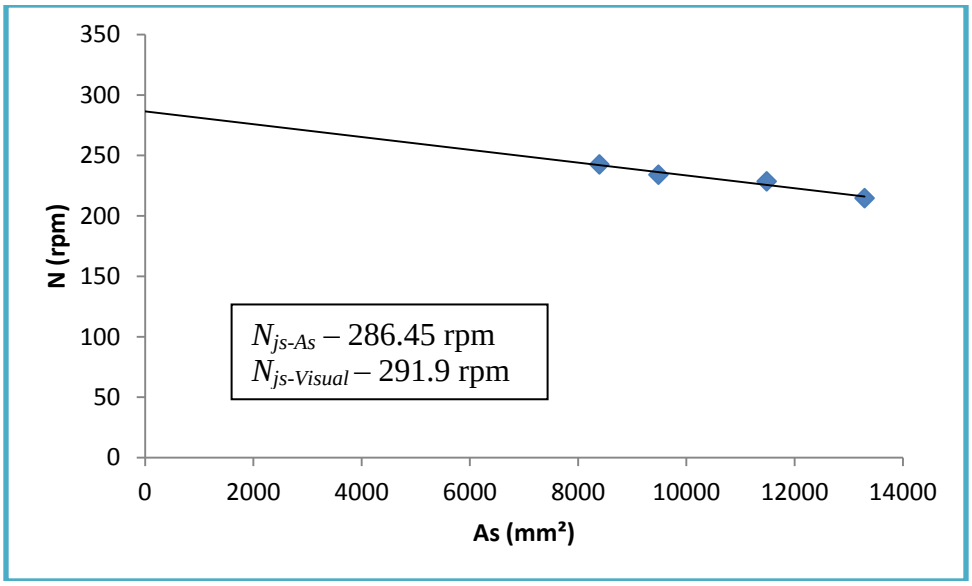

(f)

Figure 3.10 Effect of the Particle concentration on N_{js} for different impellers at varying *Cb/T* ratio: (f) PBT (150 µm Particles), *Cb/T*-0.4.

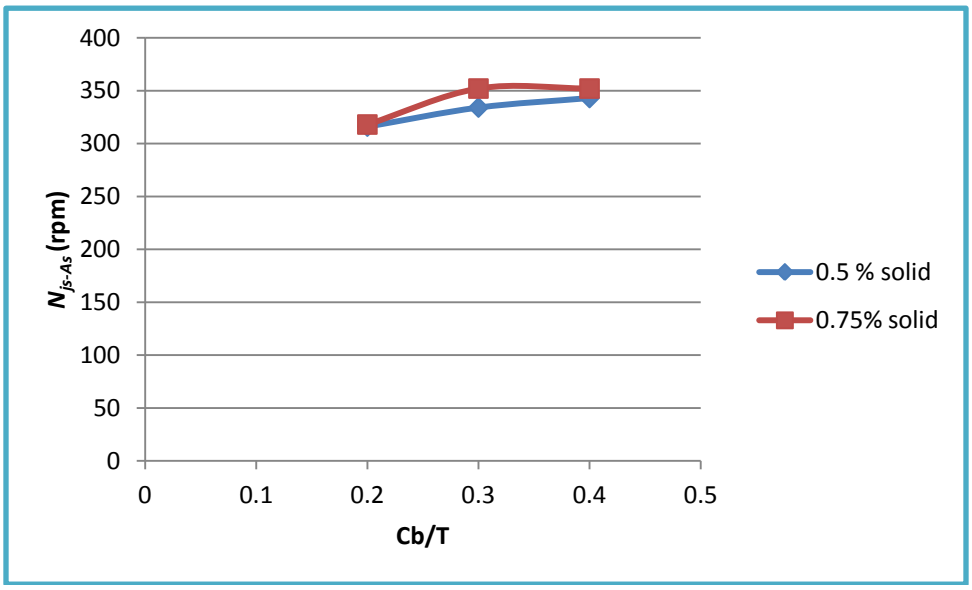

(g)

Figure 3.10 Effect of the Particle concentration on N_{js} for different impellers at varying *Cb/T* ratio: (f) DT comparison between 0.5% and 0.75% solid, for *D/T*-0.33.

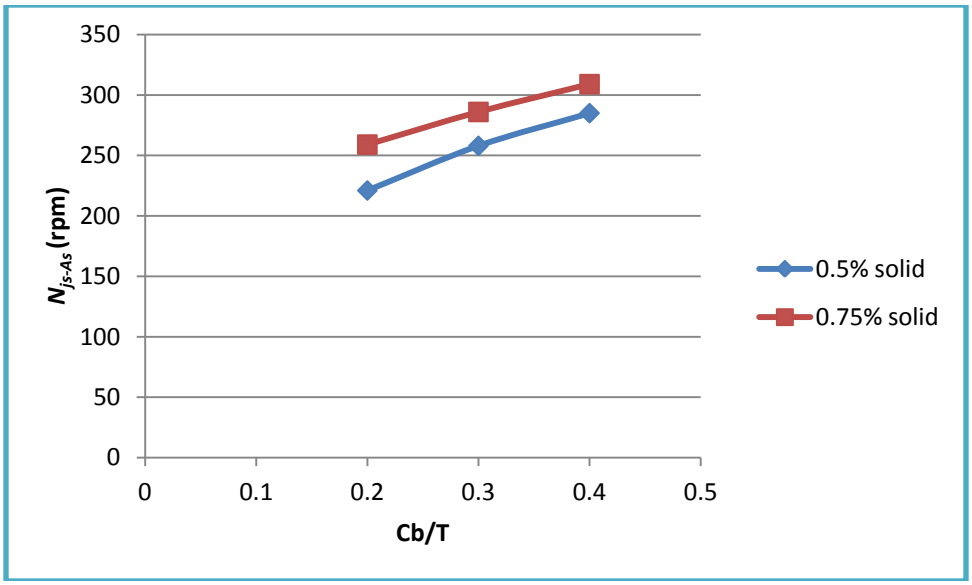

(h)

Figure 3.10 Effect of the Particle concentration on N_{js} for different impellers at varying *Cb/T* ratio: (g) PBT comparison between 0.5% and 0.75% solid, for *D/T*-0.33.

3.1.8 Effect of Tank Size on N_{js} (Scale up Effect)

Table 3.9: Results for N_{js} of largest tank, 200 µm Particles in a flat bottomed reactor

Impeller type	Particle Size (µm)	Tank Diameter (mm)	Baffling	D/T	Cb/T	$N_{js\text{-}As}$ (RPM)	$N_{js\text{-}visual}$ (RPM)
DT	200	585	FB	0.27	0.2	256	270
DT	200	585	FB	0.27	0.4	276	280
PBT	200	585	FB	0.3	0.2	276	271
PBT	200	585	FB	0.3	0.4	298	309

Table 3.8 shows N_{js} for the largest tank, which was performed in order to compare results for scale up studies. Figure 3.11 clearly indicates how the value of N_{js} differs for different sized tanks.

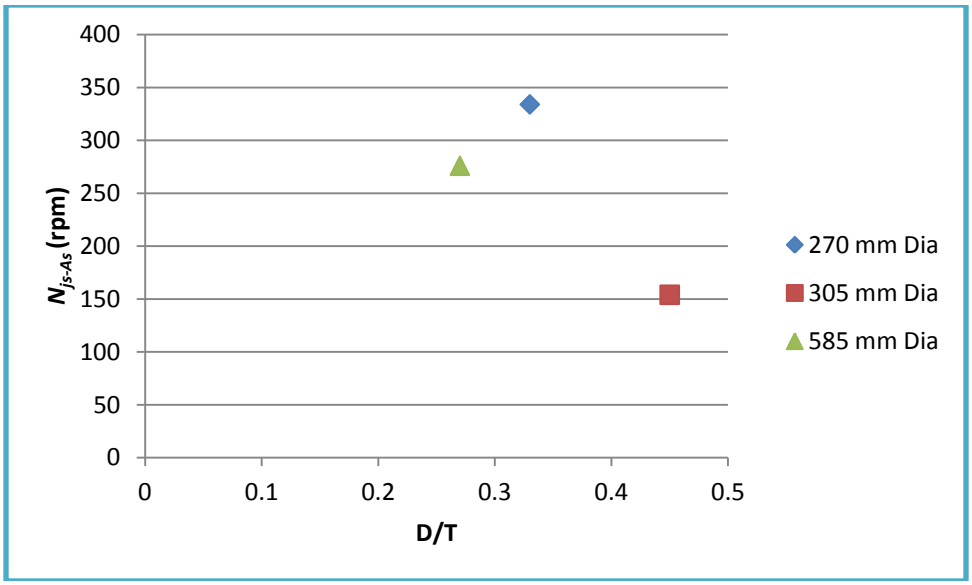

(a)

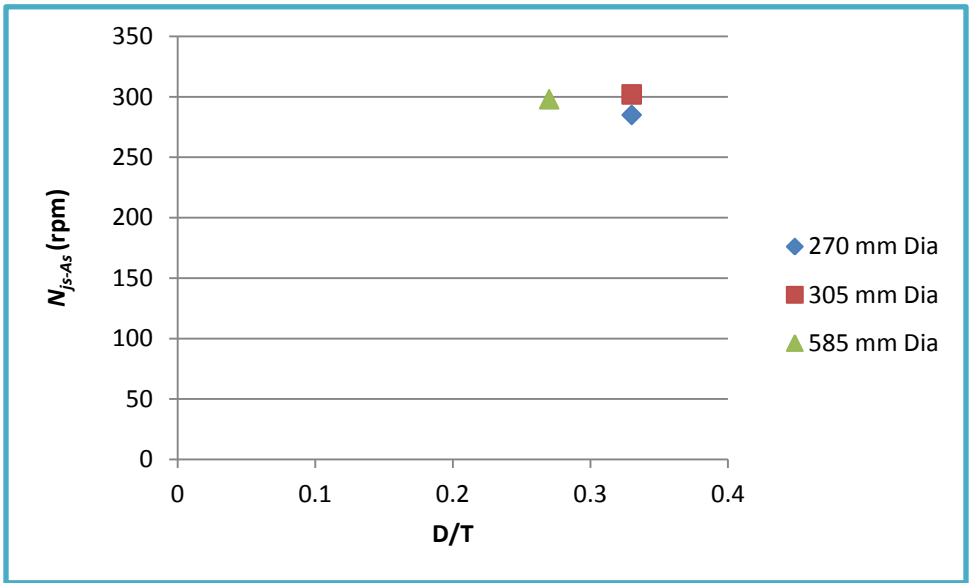

(b)

Figure 3.11 Scale up Studies on N_{js} for different impellers at varying *D/T* ratio and constant Cb/T: (a) DT (200 µm Particles) and (b) PBT (200 µm Particles).

The graph represents N_{js} at different values of Cb/T and D/T, indicating the variations of N_{js} for different sized tanks. Increase in size has of tank does not affect the N_{js} value by a lot of factor, for a constant Cb/T. Thus it clearly shows that maintaining consistent Cb/T and D/T value is important to scale up any particular process. Although there is a large

variation seen in the system where DT was used, the difference is due to the change in D/T ratio, which is a very important factor.

3.1.9 S-Value for Zwietering Equation

Based on the Zwietering Equation:

$$N_{js} = s\frac{\nu^{0.1} d_p^{0.2} \left(g\Delta\rho/\rho_L\right)^{0.45} X^{0.13}}{D^{0.85}}$$

S-value was obtained by this experiment. Figure 3.12 shows S-value vs. Njs - As for different systems. The S-value obtained is in line with the literature values, thus indicating the validity of this method.

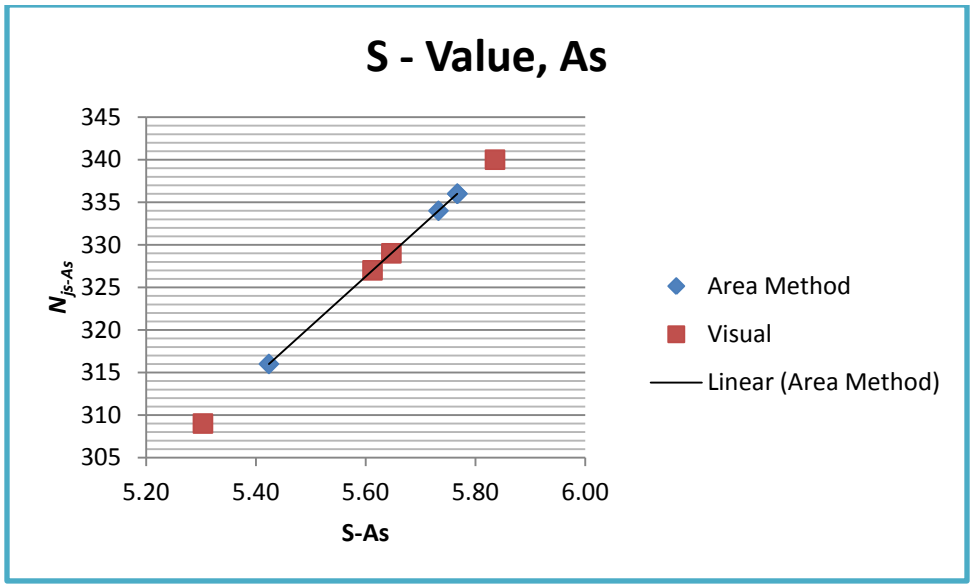

(a)

Figure 3.12 S-Value for Zwietering Equation. (a) DT (200 µm Particles).

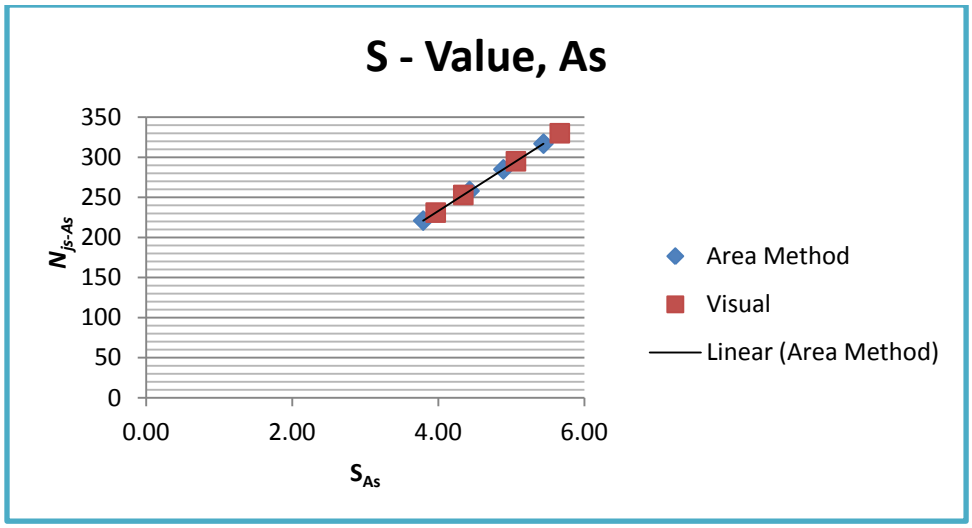

(b)

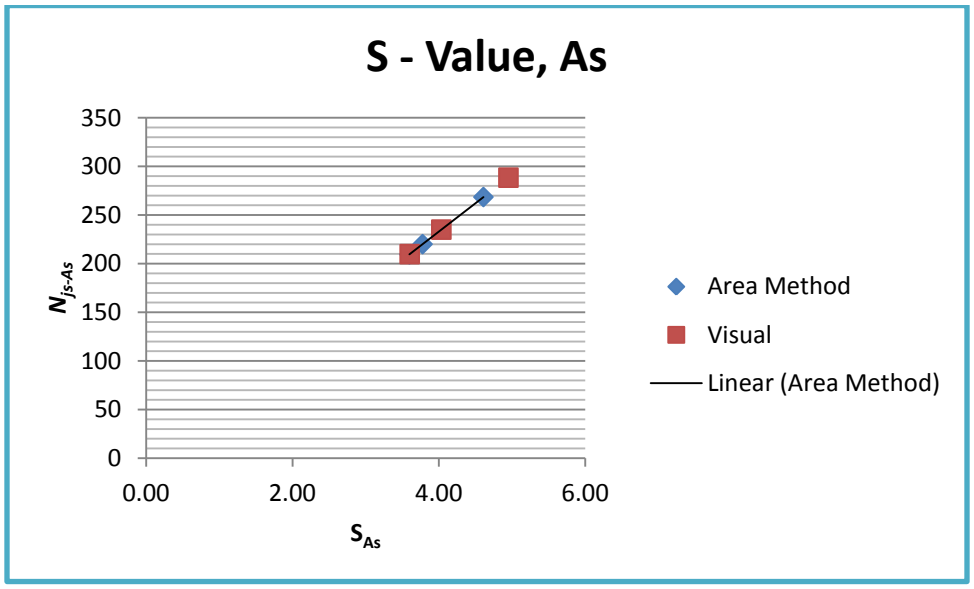

(c)

Figure 3.12 S-Value for Zwietering Equation. (b) PBT (200µm Particles); (c) FBT (200 µm Particles).

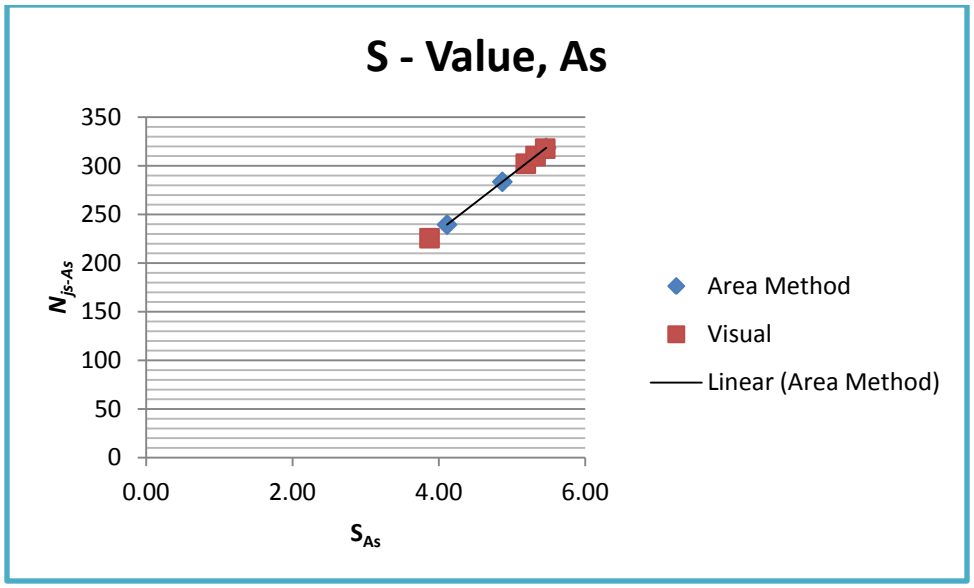

(d)

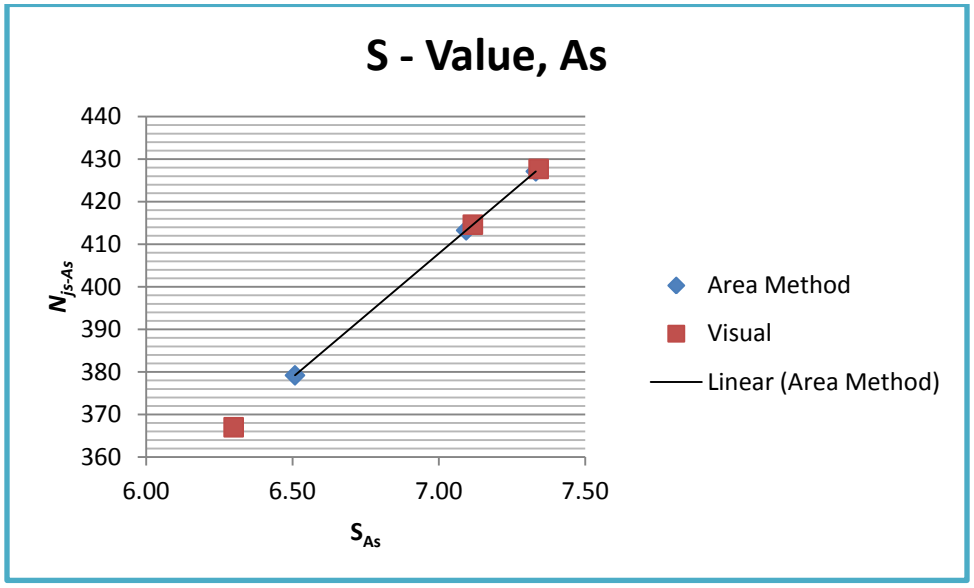

(e)

Figure 3.12 S-Value for Zwietering Equation. (d) A310 (200 µm Particles) (e) Propeller (200 µm Particles).

CHAPTER 4

CONCLUSION

In this work, the minimum agitation speed to achieve solid suspension in flat bottomed reactors commonly used in the pharmaceutical industry was experimentally obtained using five different types of impellers, i.e., 6-blade disk turbine, 6-blade pitched-blade turbine, A310 turbine, propeller and six-blade flat blade turbine under fully baffled, partially baffled and un-baffled configurations. A novel method for determination of minimum agitation speed, N_{js}, was obtained ($N_{js\text{-}As}$). The $N_{js\text{-}As}$ Method can be used for any type of system and configuration. The new method works well in the precise determination of N_{js} in flat- and hemispherical-bottomed tank systems. Triplicates experiment were conducted in most cases, and the small standard deviation for N_{js} is an indication the novel approach is highly replicable.

It was found that the value of N_{js} for the impeller under fully baffled conditions increased significantly with increasing values of C_b/T. Also increase in D/T ratio, that is increase in size of the impeller reduced the N_{js} obtained for that system. However, for the scale-up studies at various configurations and impellers, N_{js} changed only slightly with tank size.

This method was found applicable even in the case when the size and amount of solids are varied. Increase in the value of N_{js} for the increase in amount of solid was observed and decrease in N_{js} was seen when the particle size was decreased.

The results obtained in this work are directly applicable to the pharmaceutical industry where these reactors are commonly used.

APPENDIX

Table A1: S-value for DT

Impeller type	Particle Size (µm)	Tank Diameter (mm)	Baffling	D/T	Cb/T	$N_{js\text{-}As}$ (RPM)	$N_{js\text{-}visual}$ (RPM)	S - As	S - vis
DT	200	270	FB	0.33	0.2	316	309	5.42	5.30
DT	200	270	FB	0.33	0.3	334	340	5.73	5.84
DT	200	270	FB	0.33	0.4	336	327	5.77	5.61
DT	200	270	FB	0.33	0.5	336	329	5.77	5.65
DT	200	270	FB	0.22	0.3	188	192	3.23	3.30
DT	200	270	FB	0.59	0.3	119	127	2.04	2.18
DT	200	305	UB	0.45	0.3	176	188	3.02	3.23
DT	200	305	HB	0.45	0.3	146	152	2.51	2.61
DT	200	305	FB	0.45	0.3	154	162	2.64	2.78

Table A2: S-value for PBT

Impeller type	Particle Size (µm)	Tank Diameter (mm)	Baffling	D/T	Cb/T	$N_{js\text{-}As}$ (RPM)	$N_{js\text{-}visual}$ (RPM)	S - As	S - vis
PBT	200	270	FB	0.33	0.2	221	231	3.79	3.96
PBT	200	270	FB	0.33	0.3	258	253	4.43	4.34
PBT	200	270	FB	0.33	0.4	285	295	4.89	5.06
PBT	200	270	FB	0.33	0.5	317	330	5.44	5.66
PBT	200	270	FB	0.29	0.3	345	331	5.92	5.68
PBT	200	270	UB	0.33	0.3	305	333	5.23	5.72
PBT	200	305	HB	0.33	0.3	261	283	4.48	4.86
PBT	200	305	FB	0.33	0.3	302	320	5.18	5.49

Table A3: S-value for FBT

Impeller type	Particle Size (µm)	Baffling	D/T	Cb/T	$N_{js\text{-}As}$ (RPM)	$N_{js\text{-}visual}$ (RPM)	S - As	S - vis
FBT	200	FB	0.33	0.2	209.54	209.8	3.60	3.60
FBT	200	FB	0.33	0.25	220.05	235	3.78	4.03
FBT	200	FB	0.33	0.3	268.49	288.4	4.61	4.95

Table A4: S-value for A310

Impeller type	Particle Size (µm)	Baffling	D/T	Cb/T	$N_{js\text{-}As}$ (RPM)	$N_{js\text{-}visual}$ (RPM)	S - As	S - vis
A310	200	FB	0.45	0.2	283.56	302.2	4.87	5.19
A310	200	FB	0.45	0.25	314.76	317.7	5.40	5.45
A310	200	FB	0.45	0.3	318.45	310	5.47	5.32
A310	200	FB	0.55	0.3	239.54	225.6	4.11	3.87
A310	200	FB	0.33	0.3	387.36	383.6	6.65	6.58

Table A5: S-value for Propeller

Impeller type	Particle Size (µm)	Baffling	D/T	Cb/T	$N_{js\text{-}As}$ (RPM)	$N_{js\text{-}visual}$ (RPM)	S - As	S - vis
Propeller	200	FB	0.33	0.2	379.2	367	6.51	6.30
Propeller	200	FB	0.33	0.3	413.27	414.6	7.09	7.12
Propeller	200	FB	0.33	0.4	427.13	427.7	7.33	7.34

REFERENCES

1. Armenante, P.M., Uehara-Nagamine, E., "Determination of correlations to predict the minimum agitation speed for complete solid suspension in agitated vessels." *Canadian Journal of Chemical Engineering*, 76, pp. 413-419 (1998).
2. Zwietering, T. N. "Suspending solid particles in liquids by agitators." *Chem. Eng. Sci.* 8, pp. 244-253 (1958).
3. Alvin W. Nienow, Christopher J. Hewitt, Thomas R.J. Heathman,Veronica A.M. Glyn, Gonc¸alo N. Fonte, Mariana P. Hanga, Karen Coopman, Qasim A. Rafiq, " Agitation conditions for the culture and detachment of hMSCs from microcarriers in multiple bioreactors platforms." *Biochemical Engineering Journal*, BEJ – 6263.
4. Scargiali, F., Busciglio, A., Grisafi, F., Tamburini, A., Micale, G., & Brucato, A., "Power consumption in uncovered unbaffled stirred tanks: influence of viscosity and flow regime." *Industrial & Engineering Chemical Research*, 52, pp. 14998-15005 (2013).
5. S. Ibrahim, S.N. Jasnin, S.D.Wong and I.F. Baker, "Zwierering's equation for the suspension of porous particles and the use of curved blade impellers." *International Journal of Chemical Engineering*, Volume 2012, Article ID 749760.
6. Inci Ayranci, Marcio B. Machado, Adam M Madej, Jos J. Derksen, David S. Nobes, Suzanne M. Kresta. "Effect of Geometry on the mechanisms for off-bottomed solids suspension in stirred tank." *Chemical Engineering Science Journal*, page 163-176 (2012).